are involved in regulating feeding behavior and energy homeostasis in mice.

Materials and methods

Animals and drug treatment. Four-week-old male C57BL/6J mice were purchased from Japan CLEA. Mice were individually housed in cages with free access to water and chow pellets in a light- (12 h on/12 h off; lights on at 08:00 h and lights off at 20:00 h) and temperature (20–22 °C)-controlled environment. Animals were acclimatized to the laboratory environment for 1 week before the experiment. mCPP and fenfluramine were purchased from Sigma Chemical (St. Louis, MO, USA). mCPP (5 mg/kg) and fenfluramine (3 mg/kg) were dissolved in saline. Drugs were administered at 10 a.m. to12 p.m. mCPP and fenfluramine were purchased from Sigma Chemical, Japan. mCPP (5 mg/kg) and fenfluramine (3 mg/kg) were dissolved in saline. The doses of mCPP (5 mg/kg) and fenfluramine (3 mg/kg) were set on the evidence that either mCPP or fenfluramine-induced hypophagia is attenuated in 5-HT2C receptor-deficient mice [1,4].

In the first experiment, 5-week-old male C57BL/6J mice in either a fed or 24-h fasted state were decapitated and blood was collected. Whole blood was mixed with EDTA-2Na (2 mg/ml) and aprotinin (500 kIU/ml) to determine the plasma active ghrelin levels. The hypothalamus was removed for RNA extraction.

In the second experiment, 5-week-old male C57BL/6J mice were deprived of food for 23 h. The following morning, the animals were intraperitoneally injected with saline or mCPP (5 mg/kg) or fenfluramine (3 mg/kg). Sixty minutes later, the animals were decapitated and blood was drawn; the animals were not fed. The hypothalamus was removed for RNA extraction.

The animal studies were conducted under protocols in accordance with the Institutional Guidelines for Animal Experiments at Tohoku University.

Real-time quantitative RT-PCR. Total RNA was isolated from mouse hypothalamic tissue using the RNeasy Midi kit (Qiagen, Hilden, Germany) according to the manufacturer's directions, and cDNA synthesis was performed using a Super Script III First-Strand Synthesis System for RT-PCR Kit (Invitrogen, Rockville, MD) using 1 μg total RNA. cDNA synthesized from total RNA was evaluated in a real-time polymerase chain reaction (PCR) quantitative system (Light Cycler Quick System 350S; Roche Diagnostics, Mannheim, Germany). The primers used were as follows. For mouse 5-HT1B receptor, sense, 5′-TGC CTG CTG GTT TCA CAT-3′, 5′-ATA GAT GTG TGG AGC TGG TG-3′, antisense, 5′-GCG CAC TTA AAG CGT ATC A-3′; 5-HT2C receptor, sense, 5′-CTG AGG GAC GAA AGC AAA G-3′, antisense, 5′-CAC ATA GCC AAT CCA AAC AAA C-3′; pro-opiomelanocortin (POMC), sense, 5′-ATA GAT GTG TGG AGC TGG TG-3′, antisense, 5′-GGC TGT TCA TCT CCG TTG-3′; for mouse cocaine- and amphetamine-regulated transcript (CART), sense, 5′-CTG GAC ATC TAC TCT GCC GTG G-3′, antisense, 5′-GTT CCT CGG GGA CAG TCA CAC AGC-3′; for mouse neuropeptide Y (NPY), sense, 5′-GCT TGA AGA CCC TTC CAT TGG TG-3′, antisense, 5′-GGC GGA GTC CAG CCT AGT GG-3′; for mouse agouti-related protein (AGRP), sense 5′-CAG ACC GAG CAG AAG AAG-3′, antisense, 5′-GAC TCG TGC AGC CTT ACA-3′; for mouse ghrelin, sense, 5′-GAA AGG AAT CCA AGA AGC CA-3′, antisense, 5′-GCT TGA TGC CAA CAT CGA A-3′; for mouse agouti-related peptide (AGRP), sense, 5′-CAG ACC GAG CAG AAG AAG-3′, antisense, 5′-GAC TCG TGC AGC CTT ACA-3′; and for mouse β-actin, sense, 5′-TTG TAA CCA ACT GGG ACG ATA TGG-3′, antisense, 5′-GAT CTT GAT CTT CAT GGT GCT AGG-3′. The relative amount of mRNA was calculated with β-actin mRNA as the invariant control. The data are shown as the percentage of mean values of the control group which received saline.

Plasma active ghrelin assay. Plasma active ghrelin levels were measured by enzyme-linked immunosorbent assay (ELISA; Active Ghrelin ELISA kit, Mitsubishi Kagaku Iatron, Japan) according to the manufacturer's instructions. For the ELISA of active ghrelin, 1 N hydrochloric acid was added to the samples at a final concentration of 0.1 N immediately after plasma separation.

Statistical methods. Data are presented as mean values ± SEM. Statistical significance of differences between two groups was determined using Student's t test. A value of $P < 0.05$ was considered statistically significant.

Results and discussion

Hypothalamic 5-HT1B receptor and 5-HT2C receptor mRNA levels in fed and fasted mice

The hypothalamic 5-HT1B receptor mRNA levels and 5-HT2C receptor mRNA levels were significantly increased in 24-h fasted mice compared with fed mice (2-fold and 2-fold, respectively; Fig. 1A). Plasma active ghrelin levels were also significantly increased in 24-h fasted mice compared with fed mice (2.5-fold; Fig. 1B). These results indicate that increases in the expression of hypothalamic 5-HT1B receptor and 5-HT2C receptor genes are

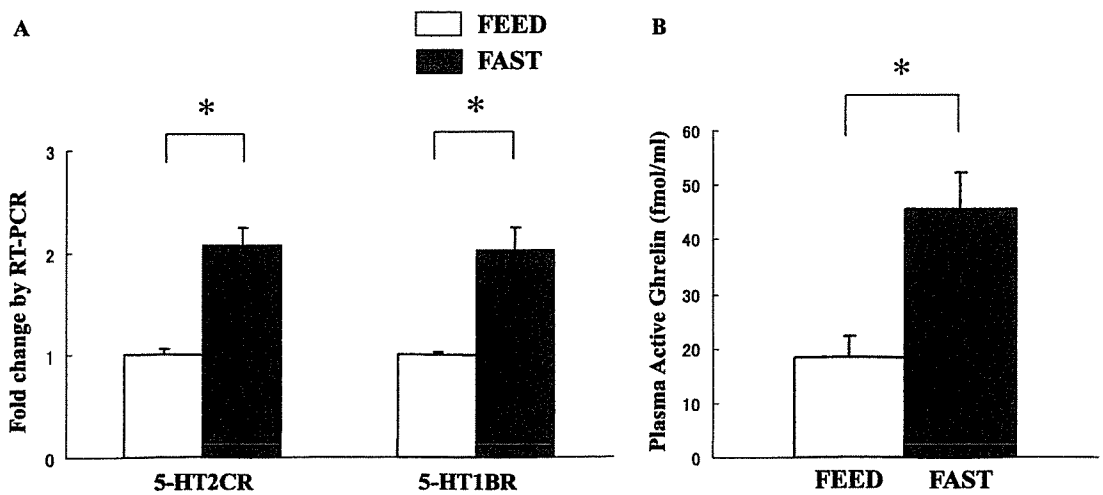

Fig. 1. Hypothalamic 5-HT2C receptor and 5-HT1B receptor mRNA levels (A) and plasma active ghrelin levels (B) in fed and 24-h fasted C57BL6J mice. Each column and bar represents the mean value ± SEM of six mice. *$P < 0.05$.

proportional to the increases in plasma active ghrelin levels after a 24-h fast.

Effects of mCPP or fenfluramine on plasma active ghrelin levels

To determine the effects of activation of brain 5-HT systems on plasma active ghrelin levels, we examined the effects of mCPP or fenfluramine on plasma levels of active ghrelin. Administration of either mCPP or fenfluramine significantly inhibited plasma active ghrelin levels after a 24-h fast (to 56% and 59% that of saline controls, respectively) (Fig. 2). These findings indicate that brain 5-HT systems via 5-HT2C receptors and/or 5-HT1B receptors play an inhibitory role in the regulation of plasma active ghrelin levels.

Effects of mCPP or fenfluramine on the expression of hypothalamic genes involved in the regulation of energy homeostasis

To determine the effects of mCPP or fenfluramine on the expression of the hypothalamic genes involved in the regulation of energy homeostasis, we examined the expression of hypothalamic POMC, CART, NPY, AGRP, and ghrelin genes that have an important role in the regulation of energy homeostasis [10,13,14]. mCPP slightly but significantly increased hypothalamic POMC and CART mRNA levels compared with saline controls (1.3- and 1.6-fold, respectively) while it had no significant effects on hypothalamic NPY, AGRP, and ghrelin mRNA levels (Fig. 3A). Fenfluramine significantly increased hypothalamic POMC and CART mRNA levels compared with saline controls (1.8- and 1.7-fold, respectively; Fig. 3B) while it had no significant effects on hypothalamic NPY, AGRP, and ghrelin mRNA levels (Fig. 3B). These results indicate that mCPP and fenfluramine increase the expression of hypothalamic POMC and CART genes without affecting the expression of hypothalamic NPY, AGRP, and ghrelin genes, and that

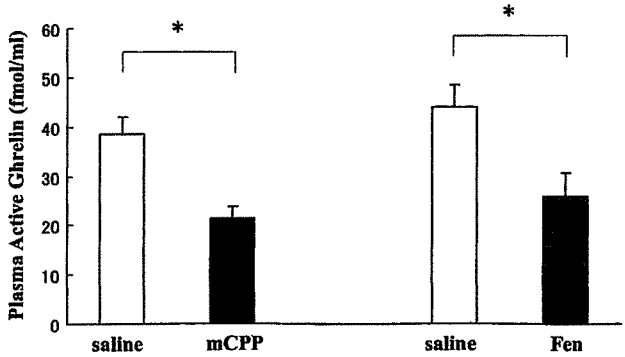

Fig. 2. Effects of mCPP (5 mg/kg) or fenfluramine (3 mg/kg) on plasma active ghrelin levels in C57BL6J mice. mCPP, fenfluramine, and saline were administered as described in Materials and methods. Each column and bar represents the mean value ± SEM of 8–12 mice. mCPP, *m*-chlorophenylpiperazine; Fen, fenfluramine. $*P < 0.05$.

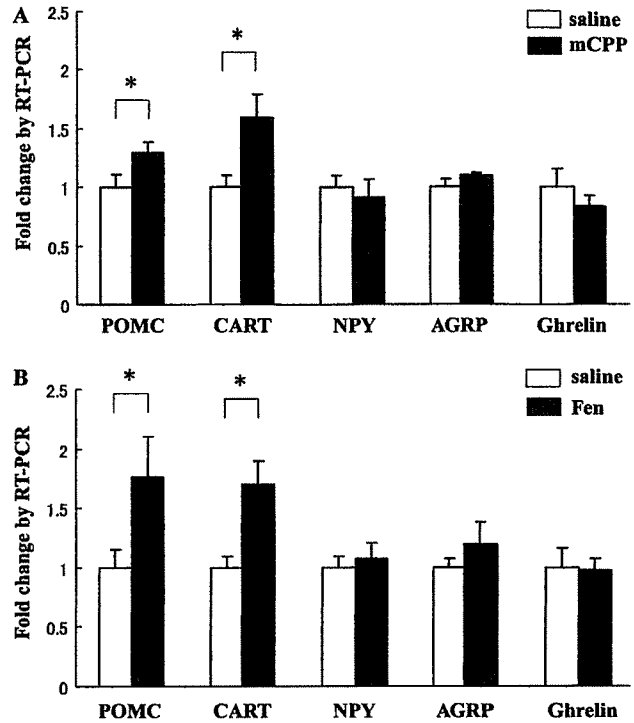

Fig. 3. Effects of mCPP (5 mg/kg) (A) or fenfluramine (3 mg/kg) (B) on hypothalamic POMC, CART, NPY, AGRP, and ghrelin mRNA levels in C57BL6J mice. mCPP, fenfluramine, and saline were administered as described in Materials and methods. Each column and bar represents the mean values ± SEM of five mice. POMC, pro-opiomelanocortin; CART, cocaine- and amphetamine-regulated transcript; NPY, neuropeptide Y; AGRP, agouti-related protein; mCPP, *m*-chlorophenylpiperazine; Fen, fenfluramine. $*P < 0.05$.

mCPP increases hypothalamic CART gene expression more than POMC gene expression.

The present results of our study demonstrate that 24-h fasting increases the expression of hypothalamic 5-HT1B receptor and 5-HT2C receptor genes associated with increases in plasma active ghrelin levels, and that mCPP and fenfluramine, which exert the anorexic effects via 5-HT2C receptors and/or 5-HT1B receptors, inhibit the increases in plasma active ghrelin levels induced by fasting. These results indicate that there is be a negative feedback system between brain 5-HT systems via 5-HT2C receptors and/or 5-HT1B receptors and plasma ghrelin levels in the regulation of energy homeostasis in mice.

Ghrelin is localized to the hypothalamic arcuate nucleus (ARC) and the stomach [10,15,16]. In the hypothalamus, ghrelin neurons contact the cell bodies and dendrites of NPY/AGRP and POMC neurons [10,16]. Hypothalamic NPY has been shown to mediate the hyperphagic action of ghrelin [17]. However, our present results demonstrate that either mCPP or fenfluramine inhibits plasma active ghrelin levels without altered the expression of hypothalamic NPY, AGRP, and ghrelin gene. Because 5-HT2C receptors are located in the central nervous system, but not the stomach [1,18], the inhibitory effects of mCPP and fenfluramine on plasma active ghrelin levels might be

mediated by the central 5-HT system. Direct effects of 5-HT on ghrelin secretion by the stomach, however, cannot be completely ruled out.

POMC neurons have been shown to express 5-HT2C receptors in the ARC [19]. POMC neurons are depolarized in response to either fenfluramine or mCPP in coronal slices of the hypothalamus of transgenic mice expressing green fluorescent protein under control of the POMC promoter [19]. The present results demonstrate that both fenfluramine and mCPP significantly increase the expression of hypothalamic POMC gene, although fenfluramine increases it more than mCPP. However, all of 5-HT2C receptors are not expressed on POMC neurons, although some of them are expressed on POMC neurons in the ARC [19]. Moreover, 5-HT2C receptors are expressed in a variety of hypothalamic nuclei other than the ARC that are involved in the regulation of feeding and energy homeostasis [18]. Accordingly, not all signals induced by the activation of 5-HT2C receptors are transferred to the melanocortin pathway.

The genes for CART, an anorexigenic peptide, are expressed in the hypothalamus, including the ARC, paraventricular nucleus, lateral hypothalamus, supraoptic nucleus, and dorsomedial nucleus of the hypothalamus [20–22]. The present results demonstrate that either mCPP or fenfluramine induces an increase in the expression of the hypothalamic CART gene, the downstream pathway of which is different from the melanocortin pathway [21–23]. Not only POMC but also CART neurons in the hypothalamus might therefore contribute to the inhibition of plasma active ghrelin levels induced by mCPP or fenfluramine.

In summary, these results suggest that there is a negative feedback system between brain 5-HT systems via 5-HT2C and/or 5-HT1B receptors and plasma active ghrelin levels, and that mCPP or fenfluramine increases the expression of hypothalamic POMC and CART genes without altering the expression of hypothalamic NPY, AGRP, and ghrelin genes in mice. This is the first report of interactions between brain 5-HT systems and plasma active ghrelin, and of the effects of activation of 5-HT systems on POMC, CART, NPY, AGRP, and ghrelin gene expression in the hypothalamus in vivo.

Acknowledgment

This work was supported by a Grant-in-Aid for Scientific Research (C2) and Human Science Research (KH21016).

References

[1] L.H. Tecott, L.M. Sun, S.F. Akana, A.M. Strack, D.H. Lowenstein, M.F. Dallman, D. Julius, Eating disorder and epilepsy in mice lacking 5-HT2C serotonin receptors, Nature 374 (1995) 542–546.

[2] K. Nonogaki, A.M. Strack, M.F. Dallman, L.H. Tecott, Leptin-independent hyperphagia and type 2 diabetes in mice with a mutated serotonin 5-HT2C receptor gene, Nat. Med. 4 (1998) 1152–1156.

[3] K. Nonogaki, L. Abdallah, E.H. Goulding, S.J. Bonasera, L.H. Tecott, Hyperactivity and reduced energy cost of physical activity in serotonin 5-HT(2C) receptor mutant mice, Diabetes 52 (2003) 315–320.

[4] S.P. Vickers, P.G. Clifton, C.T. Dourish, L.H. Tecott, Reduced satiating effect of D-fenfluramine in serotonin 5-HT(2C) receptor mutant mice, Psychopharmacology 143 (1999) 309–314.

[5] S.P. Vickers, C.T. Dourish, G.A. Kennett, Evidence that hypophagia induced by D-fenfluramine and D-norfenfluramine in the rat is mediated by 5-HT2C receptors, Neuropharmacology 41 (2001) 200–209.

[6] M.D. Lee, E.M. Somerville, G.A. Kennett, C.T. Dourish, P.G. Clifton, Reduced hypophagic effects of D-fenfluramine and the 5-HT2C receptor agonist mCPP in 5-HT1B receptor knockout mice, Psychopharmacology 176 (2004) 39–49.

[7] M. Kojima, H. Hosoda, Y. Date, M. Nakazato, H. Matsuo, K. Kangawa, Ghrelin is a growth-hormone-releasing acylated peptide from stomach, Nature 402 (1999) 656–660.

[8] M. Nakazato, N. Murakami, Y. Date, M. Kojima, H. Matuso, K. Kangawa, S. Matsukura, A role for ghrelin in the central regulation of feeding, Nature 409 (2001) 194–198.

[9] H. Ariyasu, K. Takaya, T. Tagami, Y. Ogawa, K. Hosoda, T. Akamizu, M. Suda, T. Koh, K. Natsui, S. Toyooka, G. Shirakami, T. Usui, A. Shimatsu, K. Doi, H. Hosod, M. Kojima, K. Kangawa, K. Nakao, Stomach is a major source of circulating ghrelin, and feeding state determines plasma ghrelin-like immunoreactivity levels in humans, J. Clin. Endocrinol. Metab. 86 (2001) 4753–4758.

[10] M. Kojima, K. Kangawa, Ghrelin: structure and function, Physiol. Rev. 85 (2005) 495–522.

[11] H. Hosoda, M. Kojima, H. Matsuo, K. Kangawa, Ghrelin and des-acyl ghrelin: two major forms of rat ghrelin peptide in gastrointestinal tissue, Biochem. Biophys. Res. Commun. 279 (2000) 909–913.

[12] H. Ariyasu, K. Takaya, H. Hosoda, H. Iwakura, K. Ebihara, K. Mori, Y. Ogawa, K. Hosoda, T. Akamizu, M. Kojima, K. Kangawa, K. Nakao, Delayed short-term secretory regulation of ghrelin in obese animals: evidence by a specific RIA for the active form of ghrelin, Endocrinology 143 (2002) 3341–3350.

[13] J. Korner, R.L. Leibel, To eat or not to eat—how the gut talks to the brain, N. Engl. J. Med. 349 (2003) 926–928.

[14] J.M. Friedman, Modern science versus the stigma of obesity, Nat. Med. 10 (2004) 563–569.

[15] S. Lu, J.L. Guan, Q.P. Wang, K. Uehara, S. Yamada, N. Goto, Y. Date, M. Nakazato, M. Kojima, K. Kangawa, S. Shioda, Immunocytochemical observation of ghrelin-containing neurons in the rat arcuate nucleus, Neurosci. Lett. 321 (2002) 157–160.

[16] M.A. Cowley, R.G. Smith, S. Diano, M. Tschop, N. Pronchuk, K.L. Grove, C.J. Strasburger, M. Bidlingmaier, M. Esterman, M.L. Heiman, L.M. Garcia-Segura, E.A. Nillni, P. Mendez, M.J. Low, P. Sotonyi, J.M. Friedman, H. Liu, S. Pinto, W.F. Colmers, R.D. Cone, T.L. Horvath, The distribution and mechanism of action of ghrelin in the CNS demonstrates a novel hypothalamic circuit regulating energy homeostasis, Neuron 37 (2003) 649–661.

[17] J. Kamegai, H. Tamura, T. Shimizu, S. Ishii, H. Sugihara, I. Wakabayashi, Chronic central infusion of ghrelin increases hypothalamic neuropeptide Y and agouti-related protein mRNA levels and body weight in rats, Diabetes 50 (2001) 2438–2443.

[18] D.E. Wright, K.B. Seroogy, K.H. Lundgren, B.M. Davis, L. Jennes, Comparative localization of serotonin 1A,1C and 2 receptor subtype mRNAs in rat brain, J. Comp. Neurol. 351 (1995) 357–373.

[19] L.H. Heisler, M.A. Cowley, L.H. Tecott, W. Fan, M.J. Low, J.L. Smart, M. Rubinstein, J.B. Tatro, J.N. Marcus, H. Holstege, C.E. Lee, R.D. Cone, J.K. Elmquist, Activation of central melanocortin pathways by fenfluramine, Science 297 (2002) 609–611.

[20] E.O. Koylu, P.R. Couceyro, P.D. Lambert, M.J. Kuhar, Cocaine- and amphetamine-regulated transcript peptide immunohistochemical localization in the rat brain, J. Comp. Neurol. 391 (1998) 115–132.

[21] N. Vrang, P.J. Larsen, J.T. Clausen, P. Kristensen, Neurochemical characterization of hypothalamic cocaine-amphetamine-regulated transcript neurons, J. Neurosci. 19 (1999) RC5.

[22] C.F. Elias, C.E. Lee, J.F. Kelly, R.S. Ahima, M. Kuhar, C.B. Saper, J.K. Elmquist, Characterization of CART neurons in the rat and human hypothalamus, J. Comp. Neurol. 432 (2001) 1–19.

[23] C. Broberger, Hypothalamic cocaine- and amphetamine-regulated transcript (CART) neurons: histochemical relationship to thyrotropin-releasing hormone, melanin concentrating hormone, orexin/hypocretin and neuropeptide Y, Brain Res. 848 (1999) 101–113.

Am J Physiol Endocrinol Metab 290: E308–E316, 2006.
First published September 27, 2005; doi:10.1152/ajpendo.00131.2005.

Cell type-specific activation of metabolism reveals that β-cell secretion suppresses glucagon release from α-cells in rat pancreatic islets

Rui Takahashi,[1] Hisamitsu Ishihara,[1] Akira Tamura,[1] Suguru Yamaguchi,[1] Takahiro Yamada,[1] Daisuke Takei,[1] Hideki Katagiri,[2] Hitoshi Endou,[3] and Yoshitomo Oka[1]

Divisions of [1]Molecular Metabolism and Diabetes and [2]Advanced Therapeutics for Metabolic Diseases, Tohoku University Graduate School of Medicine, Sendai, Miyagi; and [3]Department of Pharmacology and Toxicology, Kyorin University School of Medicine, Mitaka, Tokyo, Japan

Submitted 22 March 2005; accepted in final form 19 September 2005

Takahashi, Rui, Hisamitsu Ishihara, Akira Tamura, Suguru Yamaguchi, Takahiro Yamada, Daisuke Takei, Hideki Katagiri, Hitoshi Endou, and Yoshitomo Oka. Cell type-specific activation of metabolism reveals that β-cell secretion suppresses glucagon release from α-cells in rat pancreatic islets. *Am J Physiol Endocrinol Metab* 290: E308–E316, 2006. First published September 27, 2005; doi:10.1152/ajpendo.00131.2005.—Abnormal glucagon secretion is often associated with diabetes mellitus. However, the mechanisms by which nutrients modulate glucagon secretion remain poorly understood. Paracrine modulation by β- or δ-cells is among the postulated mechanisms. Herein we present further evidence of the paracrine mechanism. First, to activate cellular metabolism and thus hormone secretion in response to specific secretagogues, we engineered insulinoma INS-1E cells using an adenovirus-mediated expression system. Expression of the Na^+-dependent dicarboxylate transporter (NaDC)-1 resulted in 2.5- to 4.6-fold ($P < 0.01$) increases in insulin secretion in response to various tricarboxylic acid cycle intermediates. Similarly, expression of glycerol kinase (GlyK) increased insulin secretion 3.8- or 4.2-fold ($P < 0.01$) in response to glycerol or dihydroxyacetone, respectively. This cell engineering method was then modified, using the Cre-*loxP* switching system, to activate β-cells and non-β-cells separately in rat islets. NaDC-1 expression only in non-β-cells, among which α-cells are predominant, caused an increase (by 1.8-fold, $P < 0.05$) in glucagon secretion in response to malate or succinate. However, the increase in glucagon release was prevented when NaDC-1 was expressed in whole islets, i.e., both β-cells and non-β-cells. Similarly, an increase in glucagon release with glycerol was observed when GlyK was expressed only in non-β-cells but not when it was expressed in whole islets. Furthermore, dicarboxylates suppressed basal glucagon secretion by 30% ($P < 0.05$) when NaDC-1 was expressed only in β-cells. These data demonstrate that glucagon secretion from rat α-cells depends on β-cell activation and provide insights into the coordinated mechanisms underlying hormone secretion from pancreatic islets.

pancreatic islet; paracrine regulation; glucagon secretion; cell activation

PANCREATIC ISLETS OF LANGERHANS play a central role in glucose homeostasis. In diabetic patients, not only insulin but also glucagon secretion is impaired. Basal levels of serum glucagon are elevated, and a rise in blood glucose fails to inhibit, and can paradoxically even stimulate, glucagon release in subjects with diabetes (14). In addition, the glucagon secretory response is impaired when circulating glucose drops (11), which may result in life-threatening hypoglycemia in patients treated with insulin. This unresponsiveness to hypoglycemia makes precise glycemic management difficult (8), although strict control is known to be essential for preventing diabetic complications (38). Therefore, it is important to understand the mechanisms whereby glucagon secretion is regulated by nutrients.

Three types of regulatory mechanisms have been proposed by which nutrients, such as glucose, suppress glucagon secretion. The first is a direct action of glucose on α-cells (16, 23). Glucose metabolism in α-cells is considered to generate signals that inhibit glucagon secretion, whereas glucose metabolism increases insulin secretion in β-cells. Therefore, intracellular signaling arising from glucose metabolism might differ between the two cell types, although α-cells also express molecules essential for stimulus-secretion coupling in β-cells, including ATP-sensitive K^+ (K_{ATP}) channels (3, 5). The second mechanism involves modulation by neighboring endocrine cells, such as β- (2, 10, 13, 17, 33, 39) and δ-cells (7, 34). Several molecules, including insulin (2, 13, 33), Zn^{2+} (10, 17), γ-aminobutyric acid (GABA; see Ref. 39), and somatostatin (7, 34), have been postulated to be mediators of these inhibitory effects. Autonomic regulation is the third mechanism (6, 37) and might be clinically important for responses to hypoglycemia, although in humans the glucagon response to hypoglycemia from a transplanted (denerved) pancreas is intact, arguing against this possibility (9).

Studies of stimulus-secretion coupling in β-cells, the predominant cell type of islets, have made great progress in recent decades (20). In contrast, α-cell research has been hampered because of difficulties in getting sufficient numbers of this cell type. Nonetheless, an earlier study has found important characteristics of α-cells (32), and several recent studies have discovered interesting features of this cell type. Characterization of electrical activity and calcium dynamics revealed a unique ion channel composition in α-cells (12). In addition, pyruvate induces glucagon secretion from α-cells (17) but does not stimulate insulin secretion from β-cells. This is probably because α-cells have a transporting system for pyruvate but β-cells do not. This observation suggests that metabolized nutrients can induce exocytosis in α-cells as is the case in β-cells. However, when the pancreas is perfused or islets are stimulated with metabolized nutrients such as glucose, insulin secretion is stimulated, whereas glucagon secretion is suppressed.

Address for reprint requests and other correspondence: H. Ishihara, Div. of Molecular Metabolism and Diabetes, Tohoku Univ. Graduate School of Medicine, 2–1 Seiryo-machi, Aoba-ku, Sendai, Miyagi 980-8575, Japan (e-mail: ishihara-tky@umin.ac.jp).

The costs of publication of this article were defrayed in part by the payment of page charges. The article must therefore be hereby marked "*advertisement*" in accordance with 18 U.S.C. Section 1734 solely to indicate this fact.

In this study, to gain insight into the regulatory mechanism governing glucagon secretion in islets, we have established a method to activate cellular metabolism in β-cells and non-β-cells separately. For this purpose, we have expressed Na^+-dependent dicarboxylate transporter (NaDC)-1 or glycerol kinase (GlyK) in β-cells and/or non-β-cells. Using this method, we showed rat α-cells to secret glucagon when metabolically activated in the absence of β-cell activation. In addition, basal glucagon secretion was shown for the first time to be suppressed by β-cell activation. These data contribute to our understanding of the regulation of islet hormone secretion, providing insights that are anticipated to be of value in managing hypoglycemia and hyperglycemia in subjects with diabetes.

MATERIALS AND METHODS

Generation of recombinant adenoviruses bearing rat GlyK cDNA (AdRIPHAGlyK and AdCAGlxHAGlyKlx) and NaDC-1 cDNA (AdRIPNaDC and AdCAGlxNaDClx). Rat GlyK cDNA (31) was amplified using rat liver total RNA. An entire coding region was sequenced and subcloned downstream of the hemagglutinin (HA)-epitope sequence. Rat NaDC-1 cDNA was as described previously (36). A *Sph*I-*Spe*I fragment of HA-tagged GlyK (HAGlyK) cDNA and a *Sal*I-*Sma*I fragment of NaDC-1 cDNA were ligated between the 410-bp fragment of the rat insulin 1 promoter and the rabbit β-globin poly(A) signal region. The resulting expression units were used for generation of AdRIPHAGlyK and AdRIPNaDC by the methods described previously (27). Rat GlyK and NaDC-1 cDNA were also subcloned between two *lox*P sequences and ligated under the CAG (a transcriptional unit composed of the cytomegalovirus enhancer, the actin promoter, and the globin intron) promoter unit (28). Recombinant viruses harboring these expression units were then generated (AdCAGlxHAGlyKlx and AdCAGlxNaDClx). AdCAGlacZ (27) expressing β-galactosidase was used as a control adenovirus. AdRIPNCre was renamed from AdInsPNCre generated as described previously (17). Adenovirus titers were measured by the method described previously (27).

Isolation of rat islets and infection with recombinant adenoviruses. Rat islets were prepared by retrograde collagenase infusion through the common bile duct and hand picked under the microscope. Isolated islets were infected with the recombinant adenoviruses at 1.2×10^6 plaque-forming units (PFU)/islet in 1.0 ml medium for 60 min. In the case of combined infection of AdCAGlxNaDClx plus AdRIPNCre or AdCAGlxHAGlyKlx plus AdRIPNCre, the amount of AdRIPNCre was four times greater than the others, with a total amount of 1.2×10^6 PFU/islet.

Immunoblot analysis. INS-1E cells (25) were infected with either AdRIPHAGlyK or AdRIPNaDC at multiplicity of infection (MOI) of 100, cultured for 2 days, and directly dissolved in the SDS sample buffer. Proteins were subjected to SDS-PAGE and were transferred to nitrocellulose membranes. Membranes were probed with rabbit anti-rat NaDC-1 antibody raised against the carboxy-terminal peptide (1:500; see Ref. 36) or with anti-HA tag antibody (1:200; Santa Cruz Biotechnology, Santa Cruz, CA) for 1 h at room temperature and then incubated for 1 h with anti-rabbit IgG (1:1,000) conjugated with horseradish peroxidase, respectively. Detection was accomplished with chemiluminescence (ECL; Amersham Biosciences, Piscataway, NJ).

Immunocytochemical analyses. INS-1E cells infected with either AdRIPHAGlyK or AdRIPNaDC at an MOI of 100 were incubated with anti-rat NaDC-1 antibody (1:500) or with anti-HA tag antibody (1:200) for 1 h at room temperature and then incubated for 1 h with FITC-conjugated anti-rabbit IgG (1:500; Jackson ImmunoResearch, West Grove, PA). Islets infected with AdRIPHAGlyK, AdCAGlxHAGlyKlx alone, or AdCAGlxHAGlyKlx plus AdRIPNCre were dispersed on coverslips. Cells were then fixed with 4% paraformaldehyde and incubated with anti-HA tag antibody (1:200) followed by incubation with FITC-conjugated anti-rabbit IgG. Insulin and glucagon were also stained using mouse monoclonal antibodies against these hormones (1:1,000; Sigma-Aldrich, Tokyo, Japan) and Texas red-conjugated anti-mouse IgG (1:500; Jackson ImmunoResearch).

Hormone secretion. INS-1E cells (0.2×10^6 cells/well of 24-well plates) or islets (10 islets/tube) infected with recombinant adenoviruses were incubated over a period of 60 min in 1 ml of Krebs-Ringer-bicarbonate-HEPES buffer [140 mM NaCl, 3.6 mM KCl, 0.5 mM NaH_2PO_4, 0.5 mM $MgSO_4$, 1.5 mM $CaCl_2$, 2 mM $NaHCO_3$, 10 mM HEPES (pH 7.4), and 0.1% BSA] containing 2.5 mM glucose plus indicated stimulators. Insulin and glucagon were detected by RIA kits (Linco, St. Louis, MO).

Statistical analyses. Data are presented as means ± SE. Differences between groups were assessed by Student's *t-test* for unpaired data.

RESULTS

Expression of NaDC-1 resulted in cell activation in response to dicarboxylates. We first sought to establish a means of activating metabolism in specific cell types of pancreatic islets to study *1*) the roles of α-cell nutrient metabolism in glucagon secretion and *2*) whether activation of neighboring β-cells in response to nutrient metabolism modulates α-cell secretion. It was previously shown that β-cells expressing monocarboxylate transporter (MCT-1) metabolize pyruvate and secrete insulin in response to the monocarboxylate (18). Similarly, insulin secretion is reportedly stimulated in β-cells expressing GlyK in response to glycerol (1, 29). These data suggested that cells normally unresponsive to some nutrients can be activated by expressing protein(s) needed for their metabolism. We tested whether tricarboxylic acid (TCA) cycle intermediates alter insulin and glucagon secretion in isolated rat islets and found α-ketoglutarate, succinate, fumarate, and malate to have no effects on hormone secretion in wild-type islets (Fig. 1). A membrane-permeable analog of succinate, methylsuccinate, is known to stimulate insulin secretion (24), suggesting that inability of TCA cycle intermediates to activate β-cells is attributable to low or no expression of membrane transporters for these compounds. Therefore, to activate cells, a recombinant adenovirus harboring cDNA encoding rat NaDC-1 under the rat insulin promoter (AdRIPNaDC) was constructed, with the aim of activating the cells with TCA cycle intermediates.

We first employed rat insulinoma INS-1E cells to study whether the recombinant adenovirus induces functional expression of NaDC-1, leading to increased cellular metabolism and thereby promoting insulin secretion. Western blotting using an antibody against NaDC-1 showed strong expression of NaDC-1, with the expected protein size, in insulinoma INS-1E cells infected with AdRIPNaDC (Fig. 2*A*). Immunocytochemical analysis revealed strong staining at the cell surface, although weak staining was observed inside the cell, suggesting improper targeting of some expressed membrane proteins because of forced expression (Fig. 2*B*). As shown in Fig. 2*C*, adenovirus-mediated expression of NaDC-1 made INS-1E cells responsive to various TCA cycle intermediates. Citrate, one of the tricarboxylates, existing partly in a divalent form at pH 7.4 (36), could be transported into INS-1E cells expressing NaDC-1, and thereby induced insulin secretion. A nonmetabolizable dicarboxylate, glutarate, failed to induce insulin secretion from INS-1E cells expressing NaDC-1, indi-

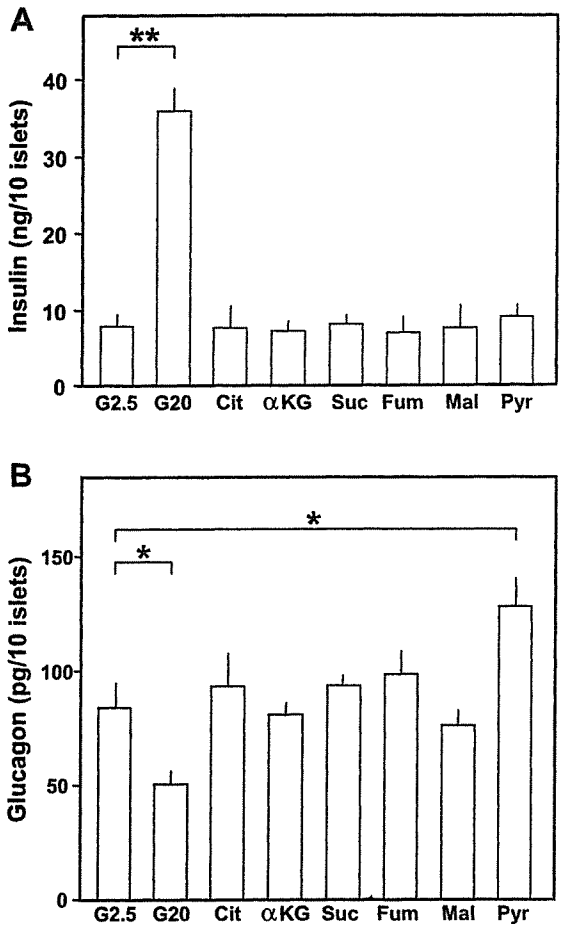

Fig. 1. Tricarboxylic acid (TCA) cycle intermediates had no effects on either insulin or glucagon secretion. Isolated islets were cultured overnight and challenged with glucose (20 mM), pyruvate (10 mM), and various TCA cycle intermediates (10 mM). Insulin (*A*) and glucagon (*B*) secreted during a 60-min incubation were measured. G2.5, 2.5 mM glucose; G20, 20 mM glucose; Cit, citrate; αKG, α-ketoglutarate; Suc, succinate; Fum, fumarate; Mal, malate; Pyr, pyruvate. Data are means ± SE; $n = 3\sim7$. $^*P < 0.05$ and $^{**}P < 0.01$.

cating insulin secretion evoked by dicarboxylates to be the result of activation of metabolism. In addition, insulin secretion evoked by malate was abolished by 2 mM NaN_3, a metabolic inhibitor (data not shown), further supporting this notion.

Expression of GlyK resulted in cell activation in response to glycerol. We also expressed rat GlyK to activate the cellular glycolytic pathway. Glycerol and dihydroxyacetone can enter the glycolytic pathway after GlyK-mediated conversion to glycerol 3-phosphate and dihydroxyacetone phosphate, respectively. Adenovirus-mediated introduction of HAGlyK cDNA resulted in expression of this protein in the INS-1E cell cytosol (Fig. 2, *D* and *E*). Expressed HAGlyK was functional, since INS-1E cells expressing HAGlyK secreted insulin in response to glycerol or dihydroxyacetone (Fig. 2*F*), as was reported in INS-1E cells expressing *Escherichia coli* GlyK (1, 29).

Taken together, these data indicate NaDC-1 and GlyK expressions to be effective in activating cellular metabolism in response to certain nutrients.

Cell type-specific expressions of genes in isolated islets. To study the stimulus-secretion coupling in α-cells and possible cross-talk with other pancreatic endocrine cells, we next sought to express the genes of interest in α- and β-cells separately. As was reported previously (17), the rat insulin 1 promoter has high transcription activity and specificity for β-cell-restricted expression of foreign genes. Therefore, β-cell-specific expression of NaDC-1 or HAGlyK was achieved using recombinant adenovirus vectors with the rat insulin 1 promoter (Fig. 3*A*). When islets were infected with AdRIPHAGlyK, >60% of insulin-positive cells were stained with HA (Fig. 3*D*), but none of the glucagon-positive cells expressed HAGlyK (Fig. 3*E*).

In contrast to the insulin 1 promoter for β-cells, the glucagon promoter (1.6 kbp) did not have high transcriptional activities specific for α-cells when placed in the adenoviral genome (data not shown). To increase expression in α-cells, a dual-adenovirus approach was previously developed (17); one adenovirus produces Cre recombinase under the glucagon promoter, and the other virus expresses the desired genes under the potent CAG promoter unit (28) once the intervening sequence is excised by Cre recombinase (17). Although the strategy increased the expression levels of reporter genes, such as luciferase, in α-cells, it did not significantly increase the activities of cellular enzymes or transporters, such as glucokinase and MCT-1 (data not shown). We then raised the recombinant virus titer. However, a high titer of virus with the glucagon promoter also induced expression in cells other than α-cells (data not shown). We therefore did not employ the glucagon promoter in this study but rather devised a method employing the insulin 1 promoter and the Cre-*loxP* system.

As shown in Fig. 3*C*, a cDNA floxed with *loxP* sequences was placed downstream from the CAG promoter unit (28) that enables transcription in any cell type. This expression unit was then introduced into islet cells, together with the insulin promoter-Cre adenovirus (AdRIPNCre; see Ref. 17). The cDNA was expected to be removed from the unit by the Cre recombinase in the β-cell, allowing expression of the genes of interest in non-β-cells, a cell population where α-cells are predominant. Indeed, when rat islets were infected with AdCAGlxHAGlyKlx and AdRIPNCre, ~70% of glucagon-positive cells was stained with HA (Fig. 3, *H* and *I*). More than 80% of HA-positive cells were observed to be stained with glucagon, and <10% were insulin positive, although HA staining was occasionally observed in somatostatin-positive cells and fibroblast-like cells (data not shown). When islets were infected with AdCAGlxHAGlyKlx alone (Fig. 3*B*), ~60% of β-cells (Fig. 3*F*) and 65% of α-cells (Fig. 3*G*) expressed HAGlyK.

α-Cell activation triggered glucagon secretion when β-cells remained nonactivated. To study the role of nutrient metabolism in glucagon secretion from α-cells, isolated rat islets were infected with AdCAGlxNaDClx plus AdRIPNCre and challenged with succinate or malate. As shown in Fig. 4, *A* and *B*, glucagon secretion was increased by 80%, without changes in insulin secretion. These effects were abolished by 2 mM NaN_3, indicating the observed glucagon secretion to be due to activation of cellular metabolism of the dicarboxylates. When islets were infected with AdCAGlxHAGlyKlx plus AdRIPNCre and then challenged with 10 mM glycerol, insulin secretion did not change (Fig. 4*C*) and glucagon secretion tended to increase, but the differences did not reach statistical significance (Fig. 4*D*).

In contrast, when α-cells were activated together with β-cells by infecting islets with AdCAGlxNaDClx alone, i.e., without AdRIPNCre (Fig. 5, *A* and *B*), insulin secretion was increased by more than threefold in response to 10 mM malate

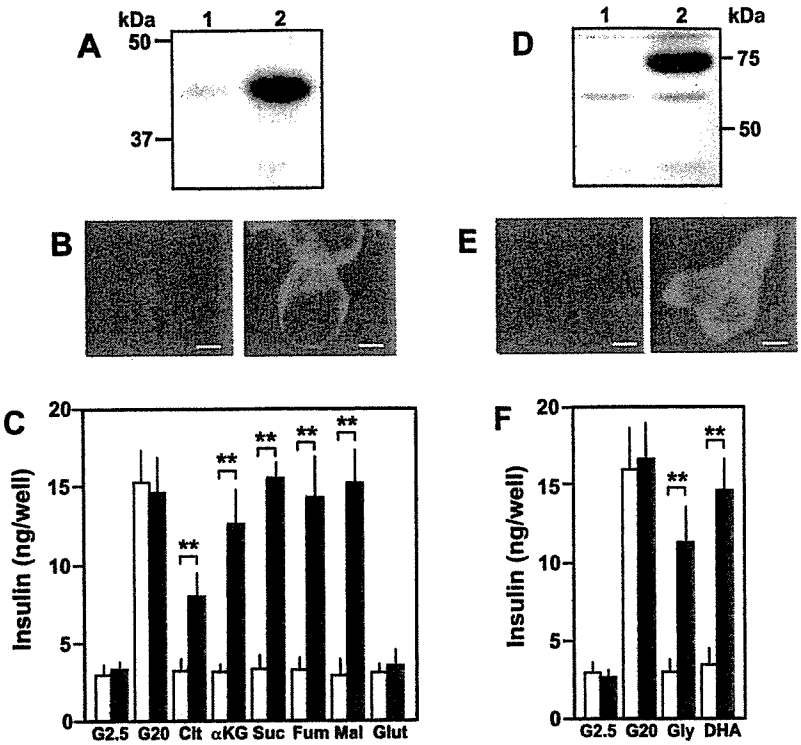

Fig. 2. Adenovirus-mediated Na^+-dependent dicarboxylate transporter (NaDC)-1 or glycerol kinase (GlyK) expression in INS-1E cells. *A*: INS-1E cells infected with either AdCAGlacZ (*lane 1*) or AdRIPNaDC (*lane 2*) were subjected to SDS-PAGE and probed with an anti-NaDC-1 antibody. *B*: INS-1E cells infected with either AdCAGlacZ (*left*) or AdRIPNaDC (*right*) were stained with anti-NaDC-1 antibody. Bars, 4 μm. *C*: INS-1E cells infected with either AdCAGlacZ (open bars) or AdRIPNaDC (filled bars) were challenged with 20 mM glucose or various TCA cycle intermediates (10 mM). Insulin secreted during a 60-min incubation was measured. Data are means ± SE; $n = 5$. $^{**}P < 0.01$. Glut, glutarate. *D*: INS-1E cells infected with either AdCAGlacZ (*lane 1*) or AdRIPHAGlyK (*lane 2*) were subjected to SDS-PAGE and probed with an anti-hemagglutinin (HA) antibody. *E*: INS-1E cells infected with either AdCAGlacZ (*left*) or AdRIPHAGlyK (*right*) were stained with an anti-HA antibody. Bars, 4 μm. *F*: INS-1E cells infected with either AdCAGlacZ (open bars) or AdRIPHAGlyK (filled bars) were challenged with 20 mM glucose, 10 mM glycerol (Gly), or 10 mM dihydroxyacetone (DHA). Insulin secreted during a 60-min incubation was measured. Data are means ± SE; $n = 4$. $^{**}P < 0.01$.

or succinate, whereas glucagon release was unchanged. Similarly, AdCAGlxHAGlyKlx infection increased insulin (by 2.5-fold) but not glucagon secretion with a 10 mM glycerol challenge (Fig. 5, *C* and *D*). These data indicate that α-cell activation dose not lead to glucagon secretion when β-cells are activated simultaneously.

Recent studies have postulated several molecules, including insulin (2, 13, 33), Zn^{2+} (10, 17), and GABA (39), as mediators of β-cell inhibitory effects on glucagon secretion. During succinate stimulation, insulin secreted from β-cells expressing NaDC-1 amounted to ~25 ng/ml (Fig. 5*A*). We therefore examined whether this amount of insulin inhibits glucagon secretion from islets expressing NaDC-1 in α- but not β-cells. As shown in Fig. 6, succinate-stimulated glucagon secretion from islets infected with AdCAGlxNaDClx plus AdRIPNCre was significantly suppressed by 25 ng/ml insulin, indicating that insulin mediates inhibitory effects of β-cells on glucagon secretion. However, the suppression seemed incomplete, sug-

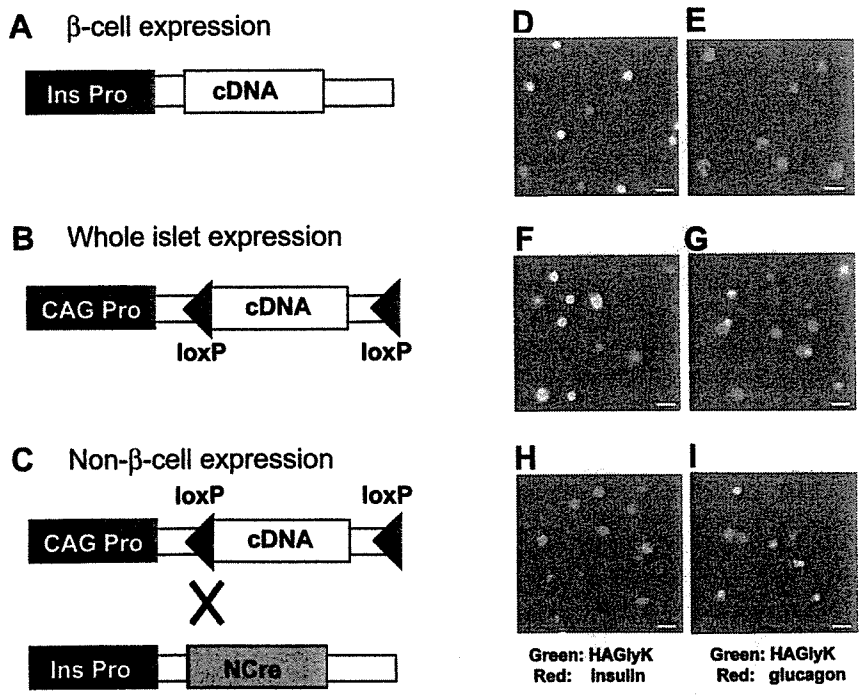

Fig. 3. Selective gene expression method for β- and non-β-cells in islets. *A–C*: schematic representation of adenoviruses for expression in β-cells (*A*), whole islet cells (*B*), and non-β-cells (*C*). NCre, nuclear targeted Cre recombinase; CAG, a transcriptional unit composed of the cytomegalovirus enhancer, the actin promoter, and the globin intron (28). *D* and *E*: islets infected with AdRIPHAGlyK were dispersed and stained with an anti-HA (green) antibody (*D* and *E*) together with anti-insulin (red; *D*) or anti-glucagon (red; *E*) antibody. *F* and *G*: islets infected with AdCAGlxHAGlyKlx alone were dispersed and stained with an anti-HA (green) antibody (*F* and *G*) together with anti-insulin (red; *F*) or anti-glucagon (red; *G*) antibody. *H* and *I*: islets infected with AdCAGlx-HAGlyKlx plus AdRIPNCre were dispersed and stained with an anti-HA (green) antibody (*H* and *I*) together with anti-insulin (red; *H*) or anti-glucagon (red; *I*) antibody. Bars, 10 μm. Colocalization resulted in yellow.

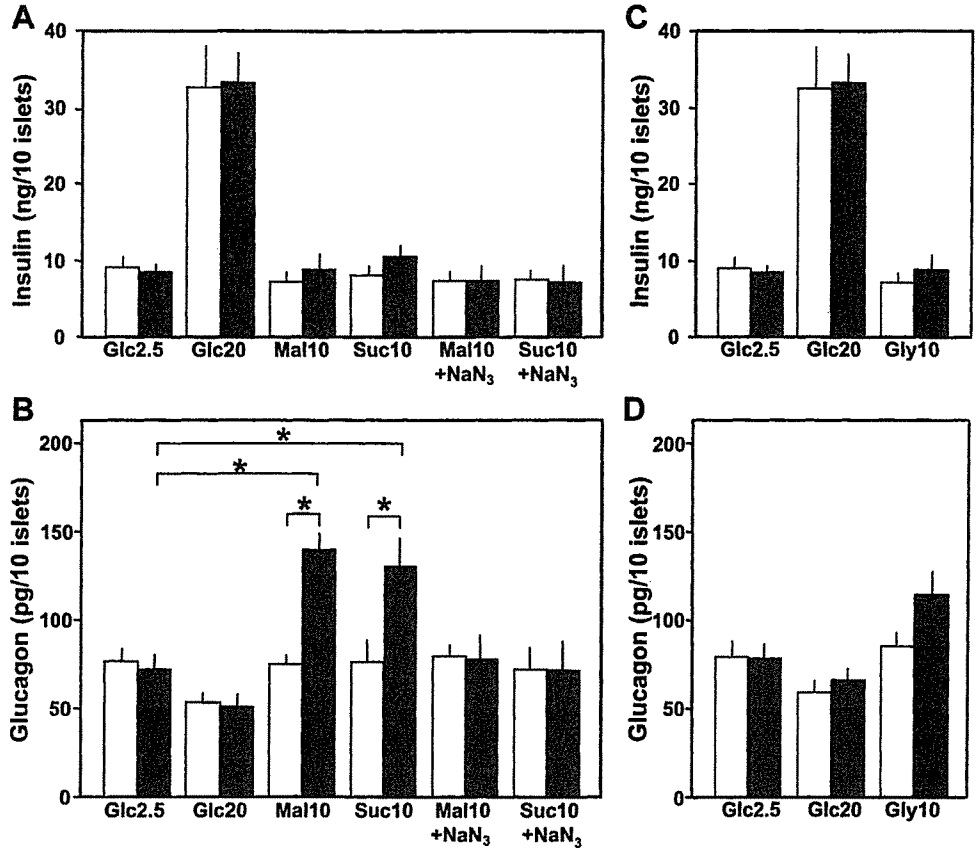

Fig. 4. Selective α-cell activation induced glucagon secretion. *A* and *B*: isolated islets (10 islets/tube) infected with AdCAGlacZ plus AdRIPNCre (open bars) or AdCAGlx-NaDClx plus AdRIPNCre (filled bars) were challenged with 20 mM glucose, 10 mM malate (Mal10), or 10 mM succinate (Suc10) with or without 2 mM NaN_3. Insulin (*A*) and glucagon (*B*) secreted during a 60-min incubation were measured; $n = 3\sim5$. $^*P < 0.05$. *C* and *D*: isolated islets (10 islets/tube) infected with AdCAGlacZ plus AdRIPNCre (open bars) or AdCAGlxHAGlyKlx plus AdRIPNCre (filled bars) were challenged with 20 mM glucose, or 10 mM glycerol (Gly10). Insulin (*C*) and glucagon (*D*) secreted during a 60-min incubation were measured; $n = 4$.

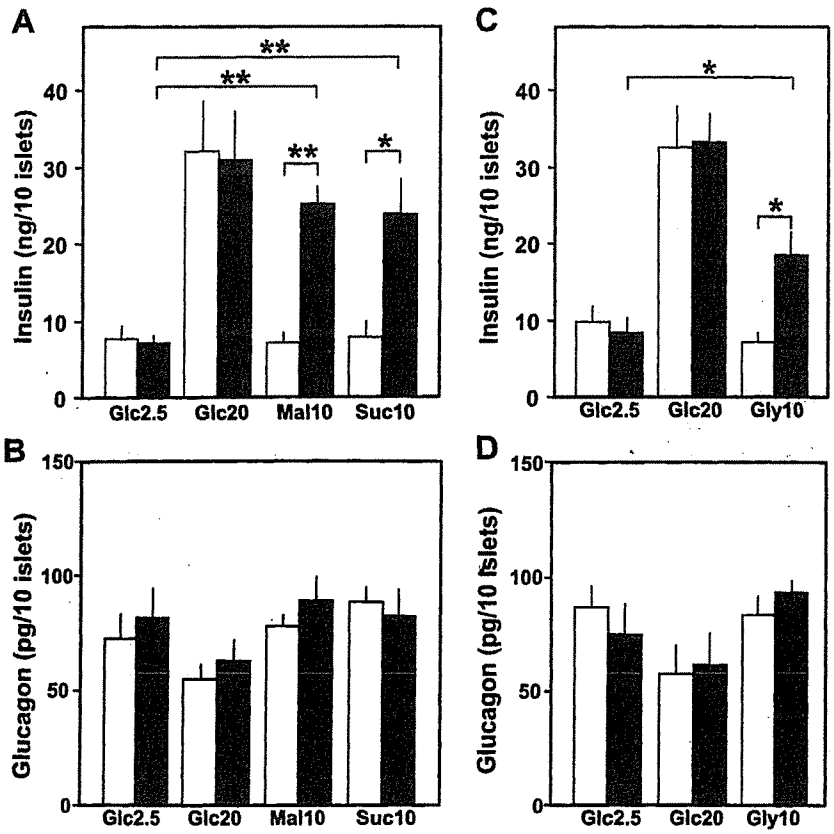

Fig. 5. Simultaneous α- and β-cell activation induced insulin but not glucagon secretion. *A* and *B*: isolated islets (10 islets/tube) infected with AdCAGlacZ (open bars) or AdCA-GlxNaDClx (filled bars) were challenged with 20 mM glucose, 10 mM malate, or 10 mM succinate. Insulin (*A*) and glucagon (*B*) secreted during a 60-min incubation were measured; $n = 4\sim6$. $^*P < 0.05$ and $^{**}P < 0.01$. *C* and *D*: isolated islets (10 islets/tube) infected with AdCAGlacZ (open bars) or AdCAGlxHAGlyKlx (filled bars) were challenged with 20 mM glucose, or 10 mM glycerol. Insulin (*C*) and glucagon (*D*) secreted during a 60-min incubation were measured; $n = 4$. $^*P < 0.05$.

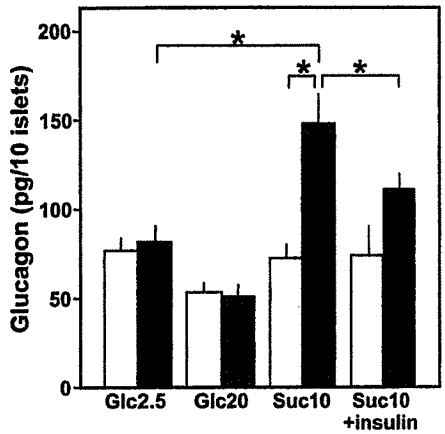

Fig. 6. Insulin suppressed succinate-stimulated glucagon secretion. Isolated islets (10 islets/tube) infected with AdCAGlacZ plus AdRIPNCre (open bars) or AdCAGlxNaDClx plus AdRIPNCre (filled bars) were challenged with 20 mM glucose, 10 mM succinate alone, or 10 mM succinate with 25 ng/ml insulin. Glucagon secreted during a 60-min incubation was measured; $n = 4$. *$P < 0.05$.

gesting another molecule(s) is also important in suppression of glucagon secretion by β-cell activation.

β-Cell activation increased insulin secretion and decreased basal glucagon secretion. We next studied whether basal glucagon secretion was altered by β-cell activation. For this purpose, NaDC-1 was expressed only in β-cells by infecting islets with AdRIPNaDC. When these islets were challenged with 10 mM malate or succinate, insulin secretion more than doubled (Fig. 7*A*). Interestingly, glucagon secretion from the same islets was reduced significantly, by 30% (Fig. 7*B*). Similar modulation of hormone secretion was observed when islets were infected with AdRIPGlyK; insulin secretion was increased significantly, by 1.7-fold, in response to 10 mM glycerol (Fig. 7*C*), whereas glucagon secretion tended to decrease, although not to a statistically significant degree (Fig. 7*D*).

DISCUSSION

Abnormal nutrient-mediated modulation of glucagon secretion is often associated with diabetes mellitus. However, the mechanisms whereby nutrients modulate glucagon secretion remain poorly understood. Paracrine modulation by β- or δ-cells is among the postulated mechanisms. Herein we provide further evidence that glucagon secretion from α-cells is stimulated by nutrient metabolism in the absence of β-cell activation but it is suppressed when β-cells are activated.

We first demonstrated, employing NaDC-1 expression, that TCA cycle intermediates induce insulin secretion from β-cells engineered to transport these substrates. It was previously reported that pyruvate and lactate stimulate insulin secretion from β-cells expressing MCT-1 and lactate dehydrogenase (LDH) but not from normal β-cells (18). This was interpreted as low levels of MCT-1 and LDH expression protecting β-cells

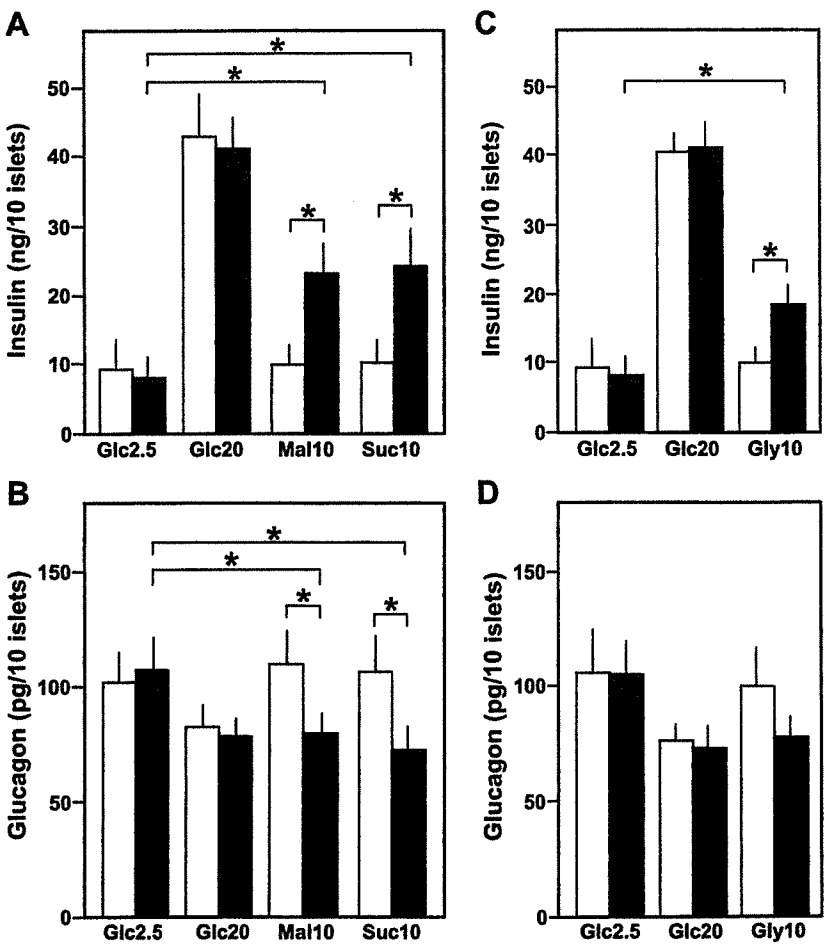

Fig. 7. Selective β-cell activation inhibited glucagon secretion. *A* and *B*: isolated islets (10 islets/tube) infected with AdCAGlacZ (open bars) or AdRIPNaDC (filled bars) were challenged with 20 mM glucose, 10 mM malate, or 10 mM succinate. Insulin (*A*) and glucagon (*B*) secreted during a 60-min incubation were measured. *$P < 0.05$; $n = 5$. *C* and *D*: isolated islets (10 islets/tube) infected with AdCAGlacZ (open bars) or AdRIPHAGlyK (filled bars) were challenged with 20 mM glucose or 10 mM glycerol. Insulin (*C*) and glucagon (*D*) secreted during a 60-min incubation were measured. *$P < 0.05$; $n = 4$.

from the stimulatory effects of pyruvate and lactate, which could otherwise cause undesired insulin secretion in catabolic states, such as during exercise. Similarly, the present data suggest that low levels of NaDC-1 expression protect β-cells from the stimulatory effects of dicarboxylates and confer glucose selectivity on insulin secretion.

A major part of the present study was based on the method we devised to activate cellular metabolism in β-cells and non-β-cells, separately, in primary rat islets by specifically expressing NaDC-1 or GlyK in β-cells and non-β-cells. Employing this innovative approach, we showed TCA cycle intermediates, succinate and malate, to induce glucagon secretion when NaDC-1 is expressed in α-cells. Stimulation of glucagon secretion was previously demonstrated in intact islets challenged with another mitochondrial substrate, pyruvate, which exerts essentially no stimulatory effects on β-cells (17). In subjects with type 1 diabetes, glucose reportedly failed to suppress, or even slightly stimulated, glucagon secretion (14). Abnormal glucagon secretion in response to glucose was also reported in islets from insulin-deficient Chinese hamsters (19). The present data, obtained employing NaDC-1 expression, thus support the concept of α-cells having an inherent capacity to increase glucagon secretion in response to nutrients under certain circumstances, i.e., in the absence of β-cell effects. GlyK expression in α-cells tended to increase glucagon secretion in response to glycerol, but not to a statistically significant degree (Fig. 3*D*). This might be because the coupling of glycolysis and mitochondrial metabolism is less efficient in α-cells than in β-cells, as previously suggested (35). In contrast, dicarboxylates directly stimulate mitochondrial metabolism in cells expressing NaDC-1, thereby possibly producing a significant increase in glucagon secretion.

The concept of α-cells having an inherent capacity to increase glucagon secretion in response to nutrients has been reinforced recently by the demonstration of glucagon secretion stimulated by glucose from purified rat α-cells (10). An earlier study (32), however, reported that glucose inhibited glucagon secretion induced by an amino acid mixture in purified α-cells. Thus direct action on α-cells could be multiple, both inhibitory and stimulatory in nature. Glucose reportedly promotes the filling of the endoplasmic reticulum Ca^{2+} stores in α-cells (23) as in β-cells (20). In the presence of an amino acid mixture, glucose inhibitory effects could attenuate the rise in cytosolic Ca^{2+} induced by amino acids, whereas glucose stimulatory effects could be masked by amino acid-stimulated Ca^{2+} elevation.

Glucagon secretion stimulated by pyruvate was previously shown to be suppressed by activation of β-cells expressing MCT-1 (17). Similar inhibition of activated glucagon secretion by β-cell secretory activities was recently reported in β-cell-specific Foxa2 knockout mice (22). Islets from these mice secreted insulin in response to an amino acid mixture, and, interestingly, the glucagon secretion that is normally seen in the wild-type islets in response to amino acids was abolished in the mutant islets. This result is consistent with the notion that suppression of activated glucagon secretion is attributable to β-cell secretory activities. In the present study, for the first time, we have shown basal glucagon secretion to also be suppressed by β-cell activation. In addition, in NaDC-1-expressing cells, glucose stimulated insulin secretion more potently (an ~4.5-fold increase) than dicarboxylates (an ~2-fold increase; Fig. 7*A*), whereas glucose and dicarboxylates suppressed glucagon secretion to a similar extent (~30%). We speculated that this is because, when islets were challenged with glucose, α-cells were also activated for glucagon secretion, which counteracted the suppressing effect exerted by β-cell secretory activities. Recent studies demonstrated that insulin (2, 13, 33), Zn^{2+} (10, 17), and GABA (39) are candidates for β-cell-derived inhibitory substances of glucagon secretion in rat islets. Our observation of inhibitory effects of insulin on succinate-stimulated glucagon secretion from islets expressing NaDC-1 in α- but not β-cells supports this notion about the role of insulin. To study roles of Zn^{2+} and GABA, it is crucial to determine amounts of these molecules secreted from β-cells during nutrient stimulation. Further studies are needed to elucidate the molecular basis of β-cell inhibitory effects.

Glucagon secretion was reported to depend differentially on Ca^{2+} influx through N- and L-type Ca^{2+} channels (12, 16). N-type Ca^{2+} channels operate predominantly under basal conditions and L-type Ca^{2+} channels in the stimulated state. β-Cell activation suppressed glucagon secretion regardless of whether α-cells were in the basal (Fig. 7*B*) or the stimulated state (Fig. 4*B*; see Refs. 17 and 22), suggesting the suppressed glucagon secretion to possibly be due to direct inhibition of two Ca^{2+} channels or to indirect inhibition of Ca^{2+} channels resulting from prevention of membrane depolarization. The latter could be achieved by opening of $GABA_A$ receptor Cl^- channels in the α-cell (39). In addition, prevention of membrane depolarization is also brought about by activation of K_{ATP} channels, which is reportedly induced by the β-cell secretory products, Zn^{2+} (4, 10) and insulin (10, 21). However, involvement of K_{ATP} channels in regulating glucagon secretion is controversial, since different glucagon responses were demonstrated in the following two mutant islets lacking functional K_{ATP} channels: preserved glucagon responses from islets deficient in one of the K_{ATP} channel subunits, Kir6.2 (26), and no response from islets deficient in another subunit, sulfonylurea receptor 1 (16).

Although inhibition of glucagon secretion by activation of β-cells expressing NaDC-1 supports the paracrine mechanism, it does not exclude a direct inhibitory effect of glucose metabolism on glucagon secretion, especially at relatively low glucose concentrations and in the presence of stimulators of glucagon secretion, such as an amino acid mixture (see above). Two different mechanisms by which glucose directly suppresses glucagon secretion have been proposed. One involves a store-operated current, which controls a depolarizing cascade leading to opening of L-type Ca^{2+} channels in α-cells (23). Thus glucose-induced ATP generation stimulates Ca^{2+} sequestration in endoplasmic reticulum and modulates a store-operated current. Another is based on low K_{ATP} channel activity and the special ion channel composition of the α-cell (5, 15); K_{ATP} channel closure by ATP produced during glucose metabolism causes modest depolarization, which inactivates, instead of activating, voltage-gated Na^+, T- and N-type Ca^{2+}, and A-type K^+ channels participating in action potential generation. Both models are based on data obtained in mouse α-cells, in which the K_{ATP} channel density is much less than

that in rat α-cells. Rat α-cells were calculated to have nearly 100-fold more K_{ATP} channels than mouse α-cells and double the number in rat β-cells (3, 5). K_{ATP} channels couple nutrient metabolism to membrane depolarization. Therefore, in rat α-cells with a greater number of K_{ATP} channels, nutrient metabolism could induce greater changes in membrane potential compared with those in mouse α-cells, thereby allowing glucagon secretion. Thus the importance of paracrine inhibition might be species dependent. It is essential to establish the level of K_{ATP} channel expression in human α-cells and whether this channel contributes to the regulation of glucagon secretion in humans. In this context, it is noteworthy that K_{ATP} channel-blocking agents stimulated glucagon secretion in subjects with insulin-deficient type 1 diabetes (30).

In summary, our findings provide further evidence supporting the concept that α-cell exocytosis can be modulated by β-cells via a paracrine mechanism. Future studies should focus on detailed molecular analyses of stimulus-secretion coupling in α-cells under paracrine regulation. This is a promising approach to identifying new drug targets for treating α-cell abnormalities in diabetic patients.

ACKNOWLEDGMENTS

We are grateful to Y. Nagura for expert assistance.

GRANTS

This work was supported by a grant from Suzuken Memorial Foundation to H. Ishihara and a Grant-in-Aid for Scientific Research (15659213) from the Ministry of Education, Science, Sports, and Culture of Japan and a Grant-in-Aid for Research on Human Genome, Tissue Engineering (H17-genome-003) from the Ministry of Health, Labor and Welfare to Y. Oka.

REFERENCES

1. **Antinozzi PA, Ishihara H, Newgard CB, and Wollheim CB.** Mitochondrial metabolism sets the maximal limit of fuel-stimulated insulin secretion in a model pancreatic β-cell: a survey of four fuel secretagogues. *J Biol Chem* 277: 11746–11755, 2002.
2. **Banarer S, McGregor VP, and Cryer PE.** Intraislet hyperinsulinemia prevents the glucagon response to hypoglycemia despite an intact autonomic response. *Diabetes* 51: 958–965, 2002.
3. **Barg S, Galvanovskis J, Gopel SO, Rorsman P, and Eliasson L.** Tight coupling between electrical activity and exocytosis in mouse glucagon-secreting α-cells. *Diabetes* 49: 1500–1510, 2000.
4. **Bloc A, Cens T, Cruz H, and Dunant Y.** Zinc-induced changes in ionic currents of clonal rat pancreatic A-cells: activation of ATP-sensitive K^+ channels. *J Physiol* 529: 723–734, 2000.
5. **Bokvist K, Olsen HL, Hoy M, Gotfredsen CF, Holmes WF, Buschard K, Rorsman P, and Gromada J.** Characterization of sulfonylurea and ATP-regulated K^+ channels in rat pancreatic A-cells. *Pflügers Arch* 438: 428–436, 1999.
6. **Burcelin R and Thorens B.** Evidence that extrapancreatic GLUT2-dependent glucose sensors control glucagon secretion. *Diabetes* 50: 1282–1289, 2001.
7. **Cejvan K, Coy DH, and Efendic S.** Intra-islet somatostatin regulates glucagon release via type 2 somatostatin receptors in rats. *Diabetes* 52: 1176–1181, 2003.
8. **Cryer PE.** Hypoglycaemia: the limiting factor in the glycaemic management of Type I and Type II diabetes. *Diabetologia* 45: 937–948, 2002.
9. **Diem P, Redmon JB, Abid M, Moran A, Sutherland DE, Halter JB, and Robertson RP.** Glucagon, catecholamine and pancreatic polypeptide secretion in type I diabetic recipients of pancreas allografts. *J Clin Invest* 86: 2008–2013, 1990.
10. **Franklin I, Gromada J, Gjinovci A, Theander S, and Wollheim CB.** β-cell secretory products activate α-cell ATP-dependent potassium channels to inhibit glucagon release. *Diabetes* 54: 1808–1815, 2005.
11. **Gerich JE, Langlois M, Noacco C, Karam JH, and Forsham PH.** Lack of glucagon response to hypoglycemia in diabetes: evidence for an intrinsic pancreatic alpha cell defect. *Science* 182: 171–173, 1973.
12. **Gopel SO, Kanno T, Barg S, Weng XG, Gromada J, and Rorsman P.** Regulation of glucagon release in mouse α-cells by K_{ATP} channels and inactivation of TTX-sensitive Na^+ channels. *J Physiol* 528: 509–520, 2000.
13. **Greenbaum CJ, Havel PJ, Taborsky GJ Jr, and Klaff LJ.** Intra-islet insulin permits glucose to directly suppress pancreatic A cell function. *J Clin Invest* 88: 767–773, 1991.
14. **Greenbaum CJ, Progeon RL, and D'Alessio DA.** Impaired β-cell function, incretin effect, and glucagon suppression in patients with type 1 diabetes who have normal fasting glucose. *Diabetes* 51: 951–957, 2002.
15. **Gromada J, Bokvist K, Ding WG, Barg S, Buschard K, Renstrom E, and Rorsman P.** Adrenalin stimulates glucagon secretion in pancreatic A-cells by increasing the Ca2+ current and the number of granules close to the L-type Ca channels. *J Gen Physiol* 100: 217–228, 1997.
16. **Gromada J, Ma X, Hoy M, Bokvist K, Salehi A, Berggren PO, and Rorsman P.** ATP-sensitive K^+ channel-dependent regulation of glucagon release and electrical activity by glucose in wild-type and $SUR1^{-/-}$ mouse α-cells. *Diabetes* 53, *Suppl* 3: S181–S189, 2004.
17. **Ishihara H, Maechler P, Gjinovci A, Herrera PL, and Wollheim CB.** Islet β-cell secretion determines glucagon secretion from the neighboring α-cells. *Nat Cell Biol* 5: 330–335, 2003.
18. **Ishihara H, Wang H, Drewes LR, and Wollheim CB.** Overexpression of monocarboxylate transporter and lactate dehydrogenase alters insulin secretory responses to pyruvate and lactate in β-cells. *J Clin Invest* 104: 1621–1629, 1999.
19. **Iwashima Y, Watanabe K, Eto M, Morikawa A, Takebe T, and Ishii K.** Insulin and glucagon response of the diabetic Chinese hamster in the Asahikawa colony. *Diabetes Res Clin Pract* 1: 87–94, 1985.
20. **Juhl K and Hutton J.** Stimulus-secretion coupling in the pancreatic β-cell. *Adv Exp Med Biol* 552: 66–90, 2004.
21. **Khan FA, Goforth PB, Zhang M, and Satin LS.** Insulin activates ATP-sensitive K(+) channels in pancreatic beta-cells through a phosphatidylinositol 3-kinase-dependent pathway. *Diabetes* 50: 2192–2198, 2001.
22. **Lantz KA, Vatamaniuk MZ, Brestelli JE, Friedman JR, Matschinsky FM, and Kaestner KH.** Foxa2 regulates multiple pathways of insulin secretion. *J Clin Invest* 114: 512–520, 2004.
23. **Liu YJ, Vieira E, and Gylfe E.** A store-operated mechanism determines the activity of the electrically excitable glucagon-secreting α-cell. *Cell Calcium* 35: 357–365, 2004.
24. **MacDonald MJ and Fahien LA.** Glyceraldehyde phosphate and methyl esters of succinic acid. Two "new" potent insulin secretagogues. *Diabetes* 37: 997–999, 1988.
25. **Merglen A, Theander S, Rubi B, Chaffard G, Wollheim CB, and Maechler P.** Glucose sensitivity and metabolism-secretion coupling studied during two-year continuous culture in INS-1E insulinoma cells. *Endocrinology* 145: 667–678, 2004.
26. **Miki T, Liss B, Minami K, Shiuchi T, Saraya A, Kashima Y, Horiuchi M, Ashcroft F, Minokoshi Y, Roeper J, and Seino S.** ATP-sensitive K+ channels in the hypothalamus are essential for the maintenance of glucose homeostasis. *Nat Neurosci* 4: 507–512, 2001.
27. **Miyake S, Makimura M, Kanegae Y, Harada S, Sato Y, Takamori K, Tokuda C, and Saito I.** Efficient generation of recombinant adenoviruses using adenovirus DNA-terminal protein complex and a cosmid bearing the full-length virus genome. *Proc Natl Acad Sci USA* 93: 1320–1324, 1996.
28. **Niwa H, Yamamura K, and Miyazaki J.** Efficient selection for high-expression transfectants with a novel eukaryotic vector. *Gene* 108: 193–199, 1991.
29. **Noel RJ, Antinozzi PA, McGarry D, and Newgard CB.** Engineering of glycerol-stimulated insulin secretion in islet β-cells. *J Biol Chem* 272: 18621–18627, 1997.
30. **Oetergard T, Degn KB, Gall MA, Carr RD, Veldhouis JD, Thomsen MK, Rizza RA, and Schmitz O.** The insulin secretagogues glibenclamide and repaglinide do not influence growth hormone secretion in humans but stimulate glucagon secretion during insulin deficiency. *J Clin Endocrinol Metab* 89: 297–302, 2004.
31. **Okamoto K, Hirano H, and Isohashi F.** Molecular cloning of rat liver glucocorticoid-receptor translocation promoter. *Biochem Biophys Res Commun* 193: 848–854, 1993.
32. **Pipeleers DG, Schuit FC, Van Schravendijk CFH, and Van de Winkel M.** Interplay of nutrients and hormones in the regulation of glucagon release. *Endocrinology* 117: 817–823, 1985.

33. **Ravier MA and Rutter GA.** Glucose or insulin, but not zinc ions, inhibit glucagon secretion from mouse pancreatic α-cells. *Diabetes* 54: 1789–1797, 2005.
34. **Schuit F, Derde MP, and Pipelers D.** Sensitivity of rat pancreatic A and B cell to somatostatin. *Diabetologia* 32: 207–212, 1989.
35. **Schuit F, DeVos A, Farfari S, Moens K, Pipelers D, Brun T, and Prentki M.** Metabolic fate of glucose in purified islet cells. *J Biol Chem* 272: 18572–18579, 1997.
36. **Sekine T, Cha SH, Hosoyamada M, Kanai Y, Watanabe N, Furuta Y, Fukuda K, Igarashi T, and Endou H.** Cloning, functional characterization, and localization of a rat renal Na^+-dicarboxylate transporter. *Am J Physiol Renal Physiol* 275: F298–F305, 1998.
37. **Taborsky GJ Jr, Ahren B, and Havel PJ.** Autonomic mediation of glucagon secretion during hypoglycemia: implications for impaired α-cell responses in type 1 diabetes. *Diabetes* 47: 995–1005, 1998.
38. **The Diabetes Control, and Complications Trial Research Group.** The effect of intensive treatment of diabetes on the development and progression of long-term complications in insulin-dependent diabetes mellitus. *N Engl J Med* 329: 977–986, 1993.
39. **Wendt A, Birnir B, Buschard K, Gromada J, Salehi A, Sewing S, Rorsman P, and Braun M.** Glucose inhibition of glucagon secretion from rat α-cells is mediated by GABA released from neighboring β-cells. *Diabetes* 53: 1038–1045, 2004.

Signals from intra-abdominal fat modulate insulin and leptin sensitivity through different mechanisms: Neuronal involvement in food-intake regulation

Tetsuya Yamada,[1,7] Hideki Katagiri,[2,7,*] Yasushi Ishigaki,[1,7] Takehide Ogihara,[2] Junta Imai,[1,2] Kenji Uno,[1,2] Yutaka Hasegawa,[1,2] Junhong Gao,[1,2] Hisamitsu Ishihara,[1] Akira Niijima,[3] Hiroyuki Mano,[4] Hiroyuki Aburatani,[5] Tomoichiro Asano,[6] and Yoshitomo Oka[1]

[1] Division of Molecular Metabolism and Diabetes
[2] Division of Advanced Therapeutics for Metabolic Diseases, Center for Translational and Advanced Animal Research
Tohoku University Graduate School of Medicine, Sendai 980-8575, Japan
[3] Niigata University School of Medicine, Niigata 951-8150, Japan
[4] Division of Functional Genomics, Jichi Medical School, Kawachi-gun, Tochigi 329-0498, Japan
[5] Research Center for Advanced Science and Technology, University of Tokyo, Tokyo 153-8904, Japan
[6] Department of Physiological Chemistry and Metabolism, University of Tokyo, Tokyo 113-8655, Japan
[7] These authors contributed equally to this work.
*Correspondence: katagiri-tky@umin.ac.jp

Summary

Intra-abdominal fat accumulation is involved in development of the metabolic syndrome, which is associated with insulin and leptin resistance. We show here that ectopic expression of very low levels of uncoupling protein 1 (UCP1) in epididymal fat (Epi) reverses both insulin and leptin resistance. UCP1 expression in Epi improved glucose tolerance and decreased food intake in both diet-induced and genetically obese mouse models. In contrast, UCP1 expression in Epi of leptin-receptor mutant mice did not alter food intake, though it significantly decreased blood glucose and insulin levels. Thus, hypophagia induction requires a leptin signal, while the improved insulin sensitivity appears to be leptin independent. In wild-type mice, local-nerve dissection in the epididymis or pharmacological afferent blockade blunted the decrease in food intake, suggesting that afferent-nerve signals from intra-abdominal fat tissue regulate food intake by modulating hypothalamic leptin sensitivity. These novel signals are potential therapeutic targets for the metabolic syndrome.

Introduction

The explosive increase in obesity has become a major public health concern in most industrialized countries (Flier, 2004; Friedman, 2003). Insulin resistance is a fundamental contributor to the metabolic syndrome associated with type 2 diabetes, hypertension, hyperlipidemia, and atherosclerosis. Major advancements in this field include the discoveries of adipocyte-derived humoral factors, such as leptin (Friedman and Halaas, 1998). Leptin conveys energy-storage information from adipose tissue to the central nervous system, leading to food-intake suppression. However, in patients with ordinary obesity, serum leptin levels are increased in proportion to body fat (Considine et al., 1996), but the responses to leptin are impaired (Heymsfield et al., 1999), which defines a state of leptin resistance. Leptin resistance also contributes to the development of obesity and obesity-related metabolic disorders.

Fat accumulation in intra-abdominal fat tissue is involved in development of the metabolic syndrome (Bjorntorp, 1992; Matsuzawa et al., 1995) associated with insulin and leptin resistance (Friedman, 2003). Therefore, in this study, to examine whether the metabolic changes in intra-abdominal fat tissue affect insulin and leptin resistance as well as systemic glucose metabolism, we attempted to express uncoupling protein 1 (UCP1), which functions to dissipate energy as heat (Klingenberg and Huang, 1999), in epididymal fat tissue (Epi) in mice with obesity and diabetes.

Results and discussion

C57BL/6 mice were subjected to direct injection of the UCP1 adenovirus vector into Epi (UCP1 mice) after the development of diabetes associated with obesity in response to high-fat chow preloading for 4 weeks. Mice given the LacZ adenovirus were used as controls (LacZ mice). Immunoblotting detected adenovirus-mediated UCP1 expression in Epi (see Figure S1A in the Supplemental Data available with this article online), and this expression was restricted to Epi (Fig. S1A). UCP1 expression in Epi was detectable on the first day after adenoviral injection and was increased on day 3 but had fallen to very low levels by day 7 (Figure S1B). However, expression levels were far below those of endogenous protein in BAT: on day 3, approximately 5% per unit weight protein (Figure S1B). UCP1 expression was restricted to very limited portions of the tissue (left panel of Figure 1B). Judging from the intensity of immunostaining, UCP1 expression levels in UCP1-expressing white adipocytes did not reach those in brown adipocytes (right panel of Figure 1B). UCP1-expressing adipocytes were significantly smaller than UCP1-nonexpressing adipocytes in the same tissue (Figure 1C), suggesting enhanced metabolism in the former.

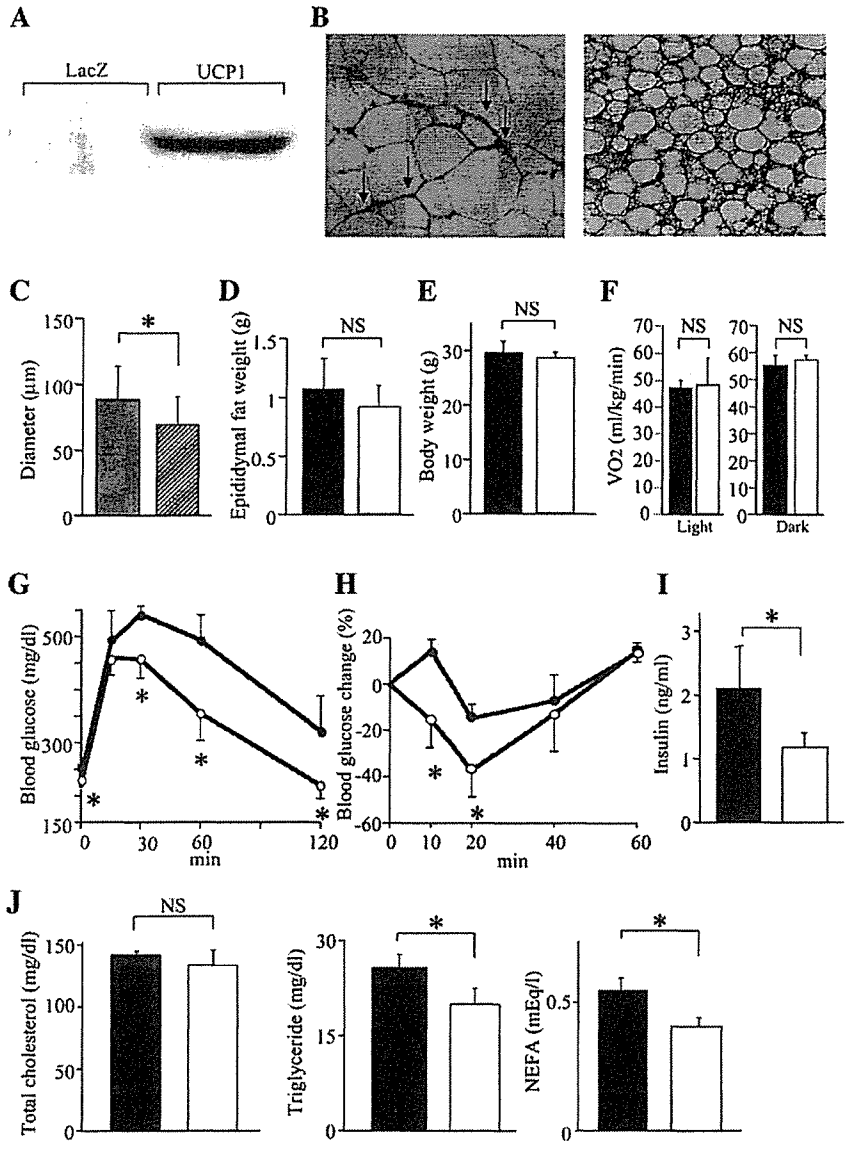

Figure 1. UCP1 expression in Epi improved glucose tolerance and insulin sensitivity

A) Immunoblotting, with anti-UCP1 antibody, of Epi extracts from LacZ and UCP1 mice on day 3 after adenoviral administration.

B) Immunohistochemistry, with anti-UCP1 antibody, of Epi (left panel) and BAT (right panel) sections from a UCP1 mouse on day 3 after adenoviral administration. These two samples were immunostained under the same conditions.

C) Diameters of UCP1-nonexpressing (gray bar) and UCP1-expressing (hatched bar) adipocytes in Epi from UCP1 mice on day 3 after adenoviral administration.

D–J) Epididymal fat weights (**D**), body weights (**E**), resting oxygen consumption during light and dark phase (**F**), and metabolic parameters (**G–J**) of LacZ mice (black bars) and UCP1 mice (white bars) on day 3 after adenoviral administration. Glucose-tolerance (**G**) and insulin-tolerance tests (**H**) were performed on day 3. Data in (**H**) are expressed as percentages of the blood glucose levels immediately before intraperitoneal insulin loading. Serum insulin levels (**I**) and serum lipid parameters ([**J**]; left: total cholesterol, middle: triglyceride, right: free fatty acids) were measured after a 10 hr fast (n = 6 per group). Data are presented as means ± SD (n = 6 per group). *$p < 0.05$ by unpaired t test.

We further confirmed enhanced metabolism by adenoviral UCP1 expression using 3T3-L1 adipocytes. UCP1 expression decreased intracellular ATP concentrations (Figure S1C) and increased levels of peroxisome proliferator-activated receptor γ coactivator (PGC) 1α and cytochrome c expression (Figure S1D). Thus, exogenous UCP1 was functionally active, resulting in increased mitochondrial biosynthesis in adipocytes.

However, neither total Epi weights nor body weights differed between LacZ and UCP1 mice on day 3 after adenoviral administration (Figures 1D and 1E). Oxygen consumption was not affected by UCP1 expression in Epi during either the light or the dark phase (Figure 1F), also reflecting the very limited UCP1 expression. Therefore, to avoid the secondary effects of body-weight change, we analyzed metabolic parameters on day 3. To our surprise, however, even very limited UCP1 expression in Epi resulted in marked changes in metabolic phenotype.

Glucose- and insulin-tolerance tests indicated marked improvements in glucose tolerance and insulin sensitivity (Figures 1G and 1H). Fasting blood glucose (Figure 1G) and insulin (Figure 1I) levels were significantly lower in UCP1 mice, further confirming improved insulin sensitivity. In addition, serum lipid parameters, including triglycerides and free fatty acids (Figure 1J), were also improved with UCP1 expression in Epi. Thus, limited regional expression of UCP1 in Epi markedly improved systemic insulin resistance, resulting in improvement of diabetes and dyslipidemia.

Next, we measured serum adipocytokine levels (Figure 2A). Adiponectin and tumor necrosis factor α levels were not significantly altered. In contrast, serum leptin was markedly decreased, by 46%, with UCP1 expression in Epi. Although intra-abdominal fat-tissue weights were unaltered or only very slightly decreased in UCP1 mice (Figure 1D and Figure S1E),

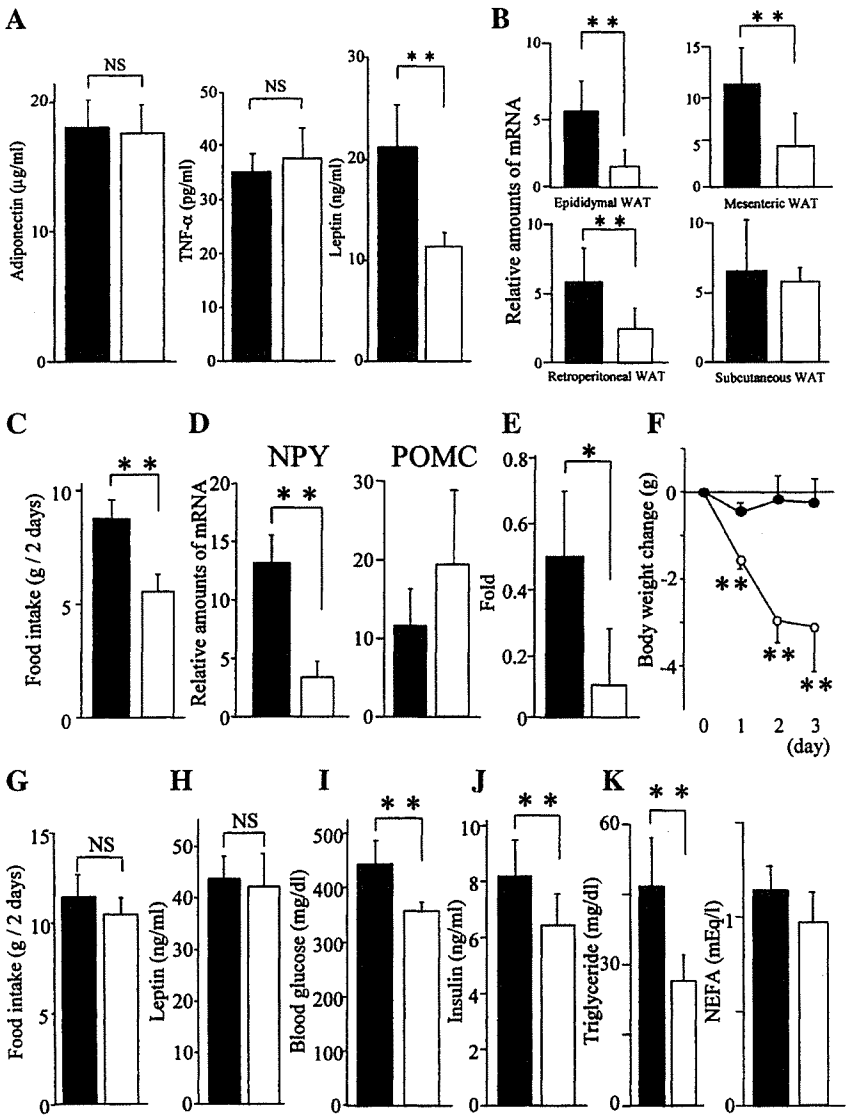

Figure 2. UCP1 expression in Epi improved leptin sensitivity

A–F) LacZ (black bars) or UCP1 (white bars) adenovirus was injected into Epi of mice with dietary obesity.

A) Serum adipocytokine levels (left: adiponectin, middle: TNFα, right: leptin) in LacZ mice and UCP1 mice after a 10 hr fast on day 3 after adenoviral administration.

B) Relative amounts of leptin mRNA in adipose tissues.

C) Total food intakes on days 2 and 3 after adenoviral administration.

D) Relative amounts of neuropeptide Y (left) and proopiomelanocortin (right) mRNA were measured by quantitative RT-PCR using total RNA obtained from the hypothalamus on day 2 after adenoviral administration. Data were corrected with β-actin as the standard (**B** and **D**).

E and F) Leptin-tolerance tests were performed on day 3 after adenoviral administration. Data were expressed as ratios to the food intakes of vehicle-treated mice (**E**). Mice were weighed at 12 hr after each daily injection of leptin or vehicle (**F**).

G–K) LacZ (black bars) or UCP1 (white bars) adenovirus was injected into Epi of db/db mice.

G) Total food intakes on days 2 and 3 after adenoviral administration are presented.

H–K) Blood leptin (**H**), glucose (**I**), and insulin (**J**) levels and serum lipid parameters ([**K**]; left: triglyceride, right: free fatty acids) of db/db mice were measured after a 10 hr fast. Data are presented as means ± SD (n = 8 per group). *p < 0.05; **p < 0.01 by unpaired t test.

leptin mRNA expression was markedly decreased in intra-abdominal fat tissues (Figure 2B). Thus, the effects of UCP1 expression in Epi are also exerted in fat tissues other than those injected with the adenovirus. Food intake was significantly suppressed (Figure 2C), indicating that hypothalamic leptin sensitivity was markedly improved despite the lack of significant changes in body weights. Decreased leptin expression in several adipose tissues suggests efferent sympathetic nerve activation, which also supports leptin signal enhancement.

Administration of green fluorescent protein-adenovirus exerted minimal metabolic effects (Figures S1F–S1J). On day 7, when adenoviral UCP1 expression was markedly decreased (Figure S1B), blood glucose, insulin, and leptin levels did not differ between the UCP1 and LacZ mice (Figure S2). In addition, we confirmed the metabolic effects of UCP1 expression in Epi using three other obese models: AKR mice on high-fat chow and KK mice and KK-Ay mice on normal chow. In these three models, similar metabolic impacts were observed with UCP1 adenovirus administration into Epi (Figure S3). Thus, UCP1 expression in Epi exerts acute, beneficial metabolic effects in both diet-induced and genetically obese models.

Increased leptin signals in the hypothalamus induced by UCP1 expression in Epi were further confirmed by changed levels of hypothalamic neuropeptide expression in UCP1 mice on day 3 after adenoviral administration. Real-time RT-PCR revealed adipose UCP1 expression to significantly decrease expression of neuropeptide Y, an orexigenic neuropeptide, while tending to increase that of proopiomelanocortin, a precursor of an anorexigenic neuropeptide, in the hypothalamus (Figure 2D).

To directly test whether leptin sensitivity was improved, we performed leptin-tolerance tests. When leptin was injected intraperitoneally into fasting mice on day 3, leptin-induced food-intake inhibition was far more profound in UCP1 mice than in LacZ mice (Figure 2E). In addition, when leptin was given daily, body weights were significantly decreased (Figure 2F). Thus,

even very limited UCP1 expression in Epi exerts a remote therapeutic effect on hypothalamic leptin resistance, which had already developed in response to preloading with high-fat chow. Transgenic overexpression of UCP1 (Kopecky et al., 1995) and rather minor induction of UCP1 in white adipose tissue (Cederberg et al., 2001; Leonardsson et al., 2004; Tsukiyama-Kohara et al., 2001; Um et al., 2004) result in resistance to high-fat-diet-induced obesity but do not reportedly cause hypophagia. In this study, however, we expressed UCP1 after the development of obesity and leptin resistance and were thus able to observe acute, beneficial effects, i.e., improved leptin sensitivity, which would be difficult to detect using congenitally UCP1-overexpressing mice.

Increased leptin sensitivity is likely to be involved in the phenotype of UCP1 mice. If this is the case, at least some of the phenotypic features of UCP1 mice would presumably be absent in mice lacking the hypothalamic leptin signal. To test this, UCP1 or LacZ adenovirus was injected into Epi of db/db mice, leptin-receptor Ob-Rb mutants. Food intake (Figure 2G) and serum leptin (Figure 2H) did not differ between LacZ-expressing and UCP1-expressing db/db mice. These findings confirm that the effect of UCP1 expression in Epi on food intake is leptin-signal dependent. On the other hand, UCP1 expression in Epi of db/db mice caused small but significant decreases in blood glucose (Figure 2I), insulin (Figure 2J), and triglyceride (Figure 2K) levels, as well as tending to decrease serum free-fatty-acid levels (Figure 2K). These findings demonstrate that UCP1 expression in Epi improves insulin sensitivity, in part, independently of leptin signaling.

To eliminate the secondary effects of reduced food intake, pair-feeding experiments were performed using C57BL/6 wild-type mice (Figure S4). Pair feeding did not significantly alter the body weights of LacZ mice. Fasting blood glucose did not differ between UCP1 mice and pair-fed LacZ mice, but after glucose loading, blood glucose levels were significantly lower in UCP1 mice. In addition, serum insulin and leptin levels were significantly lower in UCP1 mice than in pair-fed LacZ mice. Taken together with the results obtained using db/db mice, the improved insulin sensitivity induced by UCP1 expression in Epi appears not to be mediated solely by decreased food intake.

The same amounts of recombinant adenovirus encoding UCP1 were directly injected into subcutaneous fat tissues in the flank of C57BL/6 mice with dietary obesity and diabetes. UCP1 expression levels were similar to those obtained by injection into Epi (data not shown). Food intake was significantly decreased by UCP1 expression, as compared with LacZ expression, in subcutaneous fat (Figure 3A), but the effects were much smaller than those produced by UCP1 expression in Epi (Figure 2C). Furthermore, there were no statistically significant decreases in blood glucose (Figure 3B), insulin (Figure 3C), or leptin (Figure 3D) levels. Thus, exogenous UCP1 expression in subcutaneous fat was far less effective in improving insulin and leptin resistance than that in intra-abdominal fat tissue. These findings suggest the anatomical location of the manipulated adipose tissue to be involved in the observed therapeutic effects, which would appear to be important for understanding the metabolic differences between visceral fat-dominant and subcutaneous fat-dominant obesity.

How does the signal (or signals) from intra-abdominal fat tissue exert these remote effects? The importance of anatomical fat-tissue location suggests the involvement of neuronal signaling. The afferent activity from Epi is reportedly transmitted through the nerve bundle, which runs alongside blood vessels supplying Epi, in rats (Niijima, 1998). To study the possible involvement of neuronal signals from Epi, we dissected this nerve bundle in mice with dietary obesity and diabetes. Ten days after bilateral nerve-bundle dissection, adenoviruses were injected into Epi. No significant differences in body weights or Epi weights were observed between sham-operated and nerve-dissected mice (data not shown). While UCP1 adenoviral administration significantly decreased food intake in sham-operated mice, nerve dissection blunted this decrease in food intake such that it was no longer statistically significant (Figure 3E). Similarly, nerve dissection blunted a decrease in hypothalamic NPY mRNA expression, rendering it statistically insignificant (NPY; LacZ versus UCP1: 12.06 ± 6.16 versus 6.39 ± 3.10; $p = 0.15$). These findings suggest that neuronal signals from intra-abdominal fat tissue are involved in food-intake regulation. In contrast, in nerve-dissected mice, blood glucose (Figure 3F) as well as serum insulin (Figure 3G) and leptin (Figure 3H) levels were significantly suppressed in a fashion similar to in sham-operated mice. Thus, improved insulin resistance is largely independent of this neuronal pathway.

To confirm that afferent-nerve signals are involved in UCP1-expression-mediated suppression of food intake, we next examined the effects of functional deafferentation by administering capsaicin (Fu et al., 2003), a selective neurotoxin for unmyelinated C fibers. In LacZ mice, food intake was not altered by capsaicin treatment 10 days prior to adenoviral administration. In contrast, capsaicin pretreatment significantly reversed the food-intake suppression induced by UCP1 expression in Epi (Figure 3I). The inhibitory effect of capsaicin pretreatment was very similar to that of local-nerve dissection (Figure 3E). Taken together, these observations suggest that afferent-nerve signals from Epi are involved in food-intake regulation. To elucidate the molecular mechanism whereby UCP1 expression in Epi modulates neuronal activity, we searched for genes upregulated by adipose UCP1 expression. Using the DNA microarray technique, gene expressions were examined in LacZ- and UCP1-adenovirus-treated Epi (Table S1) and in 3T3-L1 adipocytes (Table S2). With the exception of UCP1, however, there was no overlap in genes showing significantly increased expression. Although further expression profiling including proteomic approaches might elucidate the underlying mechanisms, the apparent lack of genes showing increased expression raises the possibility that the activation of afferent nerves does not involve gene-expression alterations. For instance, UCP1 generates heat, and a capsaicin receptor, TRPV1, is activated by a slightly above normal body temperature (Caterina et al., 1997). Capsaicin treatment affected UCP1-induced food-intake suppression (Figure 3I), raising the possibility that UCP1 expression activates capsaicin-sensitive nerves via TRPV1 activation. Another possibility is involvement of reactive oxygen species, which are affected by mitochondrial uncoupling (Bernal-Mizrachi et al., 2005; Jezek et al., 2004) and reportedly regulate capsaicin-sensitive afferent fibers (Ruan et al., 2005). Further studies are required to examine these hypotheses.

In this study, very limited UCP1 expression in Epi markedly improved insulin and leptin resistance, thereby improving glucose tolerance and decreasing food intake. UCP1 mice were more insulin sensitive than pair-fed LacZ mice. In addition, in db/db mice, despite no food-intake suppression, blood glucose

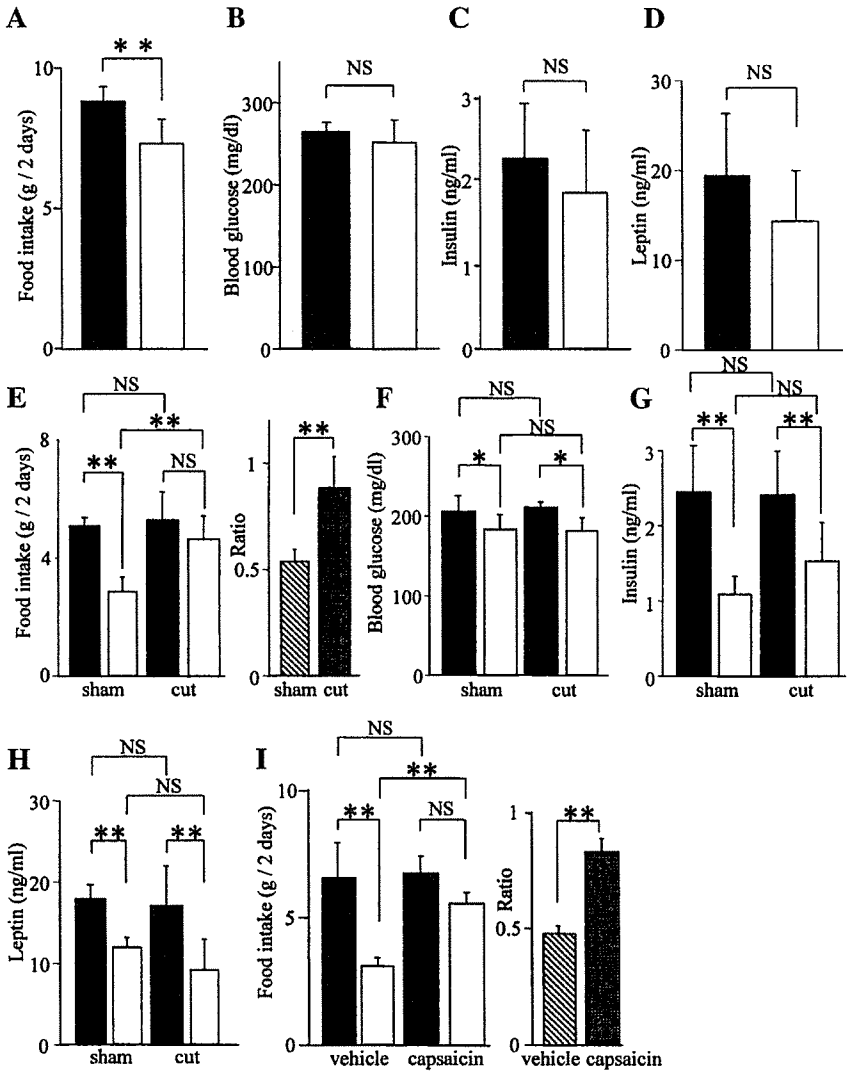

Figure 3. Neuronal signals are likely to be involved in food-intake regulation

A–D) LacZ (black bars) or UCP1 (white bars) adenovirus was injected into subcutaneous fat, and metabolic markers were measured. Total food intakes on days 2 and 3 after adenoviral administration are presented. Blood glucose (**B**), insulin (**C**), and leptin (**D**) levels were determined after a 10 hr fast on day 3 after adenoviral administration. **p < 0.01 by unpaired t test.

E–H) Mice were subjected to local-nerve dissection 10 days prior to adenoviral injection into Epi. Total food intakes of sham-operated (sham) and nerve-dissected (cut) mice (**E**) on days 2 and 3 are presented graphically. Blood glucose (**F**), serum insulin (**G**), and leptin (**H**) levels were determined on day 3.

I) Mice were treated with capsaicin or vehicle 10 days prior to adenoviral injection into Epi. Total food intakes on days 2 and 3 after administration of LacZ (black bars) or UCP1 (white bars) adenovirus are presented. In (**E**) and (**I**), the food intakes of UCP1 mice are expressed in the right graph as ratios to those of LacZ mice. **p < 0.01 assessed by one-factor ANOVA. Data are presented as means ± SD.

and insulin levels were modestly but significantly decreased by UCP1 expression in Epi. Thus, the mechanism underlying improved insulin sensitivity with UCP1 expression in Epi is, in part, independent of leptin signaling and food-intake suppression (Figure 4). Dissection of the nerve bundle from Epi did not alter the decreases in blood glucose and insulin levels. Taken together with the findings that UCP1 expression in subcutaneous fat did not significantly decrease blood glucose or insulin levels, our observations indicate that nonneuronal signals including humoral factors from intra-abdominal adipose tissue possibly participate in systemic improvement of insulin resistance. Since UCP1 expression was observed in a very limited population of adipocytes in Epi, suppression of insulin-resistant adipocytokine secretion is unlikely to explain the beneficial effects. Serum adiponectin levels were not altered, suggesting involvement of other unknown insulin-sensitizing factor (or factors).

On the other hand, decreased food intake is likely to be, at least partially, mediated by afferent-nerve signals from Epi (Figure 4). Afferent-nerve signals from Epi to the central nervous system reportedly result in a reflex from epididymal fat to white adipose tissues via efferent sympathetic-nerve activation (Niijima, 1998; Tanida et al., 2000). In addition, vagal afferent

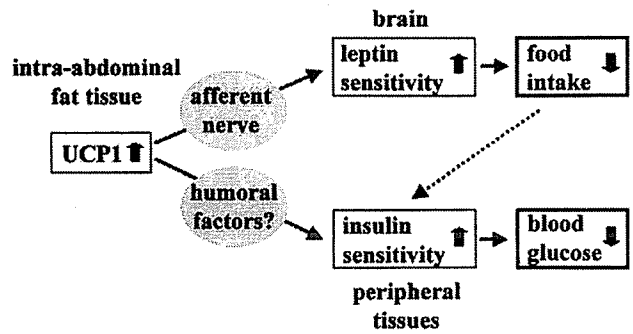

Figure 4. The proposed mechanism whereby UCP1 expression in Epi decreases food intake and improves glucose tolerance

neuronal signals from intra-abdominal tissues, including the gut (Fu et al., 2003; Smith et al., 1981) and the liver (Friedman, 1998; Scharrer, 1999), are known to play a part in regulating food intake. We also reported that UCP1 gene administration into the liver modulates food intake (Ishigaki et al., 2005). Herein we report that intra-abdominal fat tissue is likely to convey metabolic signals to the brain via a neuronal pathway, in addition to via the circulation, resulting in modulation of food intake. Although the precise molecular mechanism remains to be elucidated, this neuronal pathway might play a role in development of the metabolic syndrome, making it a potentially novel therapeutic target.

Experimental procedures

Preparation of recombinant adenovirus

Recombinant adenovirus containing murine UCP1 cDNA (Ishigaki et al., 2005) was constructed as described previously (Katagiri et al., 1996). Recombinant adenoviruses bearing the bacterial β-galactosidase gene (*Adex1CAlacZ*) and green fluorescent protein (AdCMV-GFP) were used as controls.

Animals and in vivo adenovirus injection into fat pad

Animal studies were conducted in accordance with the institutional guidelines for animal experiments at Tohoku University. Male C57BL/6N and AKR/N mice were housed individually, and high-fat-chow feeding (32% safflower oil, 33.1% casein, 17.6% sucrose, and 5.6% cellulose) (Ishigaki et al., 2005) was initiated at 5 weeks of age. After 4 weeks of high-fat-chow loading, body-weight-matched mice were anesthetized prior to dissection of the skin and body wall. The adenoviral preparation (1×10^8 plaque-forming units in a volume of 20 μl) was injected at two points each on each side of the epididymal fat pad or subcutaneous fat tissues in the flank, i.e., a total of four points. KK mice and KK-Ay mice maintained on a standard diet (65% carbohydrate, 4% fat, 24% protein) were similarly administered adenoviruses at 9 weeks and 5 weeks of age, respectively.

Immunoblotting

Tissue protein extracts (250 μg total protein) were boiled in Laemmli buffer containing 10 mM dithiothreitol, subjected to SDS-polyacrylamide gel electrophoresis, and transferred onto nitrocellulose filters. The filters were incubated with anti-UCP1 antibody (Santa Cruz Biotechnology, Santa Cruz, California) and then with anti-goat immunoglobulin G coupled to horseradish peroxidase. The immunoblots were visualized with an enhanced chemiluminescence detection kit (Amersham, Buckinghamshire, UK). The intensities of bands were quantified with the NIH Image 1.62 program.

Histological analysis

Mouse epididymal fat and BAT were immunostained as previously reported (Ishigaki et al., 2005). Mature white adipocytes were identified by their characteristic unilocular appearance. Diameters of 100 or more white adipocytes per mouse in each group were traced manually and analyzed.

Oxygen consumption

Oxygen consumption was measured as previously reported (Ishigaki et al., 2005).

Pair-feeding experiments

Pair-feeding experiments were performed as previously described (Ishigaki et al., 2005).

Blood analysis

Blood glucose and serum insulin, leptin, adiponectin, TNFα, total cholesterol, triglyceride, and free-fatty-acid levels were determined as previously described (Ishigaki et al., 2005).

Measurement of quantitative RT-PCR-based gene expression

The skull was reflected from the brain and the hypothalamus was isolated by snap freezing in liquid nitrogen as previously reported (Bjorbaek et al., 1998). Total RNA was isolated from mouse hypothalamus, fat tissues, or 3T3-L1 adipocytes with ISOGEN (Wako Pure Chemical Co., Osaka, Japan), and cDNA synthesized from total RNA was evaluated with a real-time PCR quantitative system (Light Cycler Quick System 350S; Roche Diagnostics GmbH, Mannheim, Germany).The relative amount of mRNA was calculated with β-actin mRNA as the invariant control. The primers used are shown in Table S3.

Glucose-, insulin-, and leptin-tolerance tests

Glucose-tolerance tests were performed on fasted (10 hr, daytime) mice. Mice were given glucose (2 g/kg of body weight) intraperitoneally, followed by measurement of blood glucose levels. Insulin-tolerance tests were performed on ad libitum-fed mice. Mice were intraperitoneally injected with human regular insulin (0.75 U/kg of body weight; Eli Lilly Co., Kobe, Japan).

Leptin-tolerance tests were carried out as described in a previous report (Igel et al., 1997), with slight modification. Fasted (12 hr) mice were injected with mouse leptin (7.2 mg/kg of body weight; R&D Systems, Inc.) intraperitoneally, and food intakes were monitored for 12 hr after the injection. To examine effects on body-weight change, these two groups of mice were given leptin daily starting on the day of adenoviral administration. Each mouse was then weighed.

Capsaicin treatments

Capsaicin treatment was performed as described in a previous report (Fu et al., 2003), with minor modification. Mice were anesthetized prior to subcutaneous injection of capsaicin solution (50 mg/kg, 12.5 mg/ml dissolved in vehicle). The control group received vehicle treatment (10% Tween 80, 10% ethanol, and 80% saline) under identical administration conditions. Adenoviral administration into Epi was carried out 10 days later.

Local-nerve dissection

The small nerve bundle which runs along side blood vessels supplying Epi was dissected as previously reported (Niijima, 1998). Ten days after bilateral dissection of this nerve bundle, adenoviruses were injected into epididymal fat pad.

Measurement of ATP

Fully differentiated 3T3-L1 adipocytes were infected with recombinant adenoviruses as previously described (Katagiri et al., 1996). Intracellular ATP levels were measured using an ATP determination kit (TOYO B-Net, Tokyo, Japan).

Microarray experiments

Total RNA from epididymal fat or 3T3-L1 adipocytes was used to synthesize cRNA, which was then hybridized to an HG-U133A oligonucleotide array (Affymetrix, Santa Clara, California) according to standard protocols, as described previously (Hippo et al., 2002).

Statistical analysis

All data were expressed as means ± SD. The statistical significance of differences was assessed by the unpaired t test and one-factor ANOVA.

Supplemental data

Supplemental Data include four figures and three tables and can be found with this article online at http://www.cellmetabolism.org/cgi/content/full/3/3/223/DC1/.

Acknowledgments

We appreciate Drs. L.P. Kozak (Pennington Biomedical Research Center) and H. Mizuguchi (National Institute of Biomedical Innovation) for the generous gifts of UCP1 cDNA and GFP-adenovirus, respectively. We thank Ms. H. Meguro (Tokyo University) for technical support. This work was supported by a Grant-in-Aid for Scientific Research (B2, 15390282) and a Grant-in-Aid for Exploratory Research (15659214) to H.K. from the Ministry of Education, Science, Sports and Culture of Japan and a Grant-in-Aid for Scientific Research (H16-genome-003) to Y.O. from the Ministry of Health, Labor and Welfare of Japan. This work was also supported by the 21st Century COE Programs "CRESCENDO" (H.K.) and "the Center for Innovative Therapeutic Development for Common Diseases" (Y.O.) of the Ministry of Education, Science, Sports and Culture.

Received: June 22, 2005
Revised: October 12, 2005
Accepted: February 1, 2006
Published: March 7, 2006

References

Bernal-Mizrachi, C., Gates, A.C., Weng, S., Imamura, T., Knutsen, R.H., DeSantis, P., Coleman, T., Townsend, R.R., Muglia, L.J., and Semenkovich, C.F. (2005). Vascular respiratory uncoupling increases blood pressure and atherosclerosis. Nature *435*, 502–506.

Bjorbaek, C., Elmquist, J.K., Frantz, J.D., Shoelson, S.E., and Flier, J.S. (1998). Identification of SOCS-3 as a potential mediator of central leptin resistance. Mol. Cell *1*, 619–625.

Bjorntorp, P. (1992). Abdominal fat distribution and disease: an overview of epidemiological data. Ann. Med. *24*, 15–18.

Caterina, M.J., Schumacher, M.A., Tominaga, M., Rosen, T.A., Levine, J.D., and Julius, D. (1997). The capsaicin receptor: a heat-activated ion channel in the pain pathway. Nature *389*, 816–824.

Cederberg, A., Gronning, L.M., Ahren, B., Tasken, K., Carlsson, P., and Enerback, S. (2001). FOXC2 is a winged helix gene that counteracts obesity, hypertriglyceridemia, and diet-induced insulin resistance. Cell *106*, 563–573.

Considine, R.V., Sinha, M.K., Heiman, M.L., Kriauciunas, A., Stephens, T.W., Nyce, M.R., Ohannesian, J.P., Marco, C.C., McKee, L.J., Bauer, T.L., et al. (1996). Serum immunoreactive-leptin concentrations in normal-weight and obese humans. N. Engl. J. Med. *334*, 292–295.

Flier, J.S. (2004). Obesity wars: molecular progress confronts an expanding epidemic. Cell *116*, 337–350.

Friedman, J.M. (2003). A war on obesity, not the obese. Science *299*, 856–858.

Friedman, J.M., and Halaas, J.L. (1998). Leptin and the regulation of body weight in mammals. Nature *395*, 763–770.

Friedman, M.I. (1998). Fuel partitioning and food intake. Am. J. Clin. Nutr. *67*, 513S–518S.

Fu, J., Gaetani, S., Oveisi, F., Lo Verme, J., Serrano, A., Rodriguez De Fonseca, F., Rosengarth, A., Luecke, H., Di Giacomo, B., Tarzia, G., and Piomelli, D. (2003). Oleylethanolamide regulates feeding and body weight through activation of the nuclear receptor PPAR-alpha. Nature *425*, 90–93.

Heymsfield, S.B., Greenberg, A.S., Fujioka, K., Dixon, R.M., Kushner, R., Hunt, T., Lubina, J.A., Patane, J., Self, B., Hunt, P., and McCamish, M. (1999). Recombinant leptin for weight loss in obese and lean adults: a randomized, controlled, dose-escalation trial. JAMA *282*, 1568–1575.

Hippo, Y., Taniguchi, H., Tsutsumi, S., Machida, N., Chong, J.M., Fukayama, M., Kodama, T., and Aburatani, H. (2002). Global gene expression analysis of gastric cancer by oligonucleotide microarrays. Cancer Res. *62*, 233–240.

Igel, M., Becker, W., Herberg, L., and Joost, H.G. (1997). Hyperleptinemia, leptin resistance, and polymorphic leptin receptor in the New Zealand obese mouse. Endocrinology *138*, 4234–4239.

Ishigaki, Y., Katagiri, H., Yamada, T., Ogihara, T., Imai, J., Uno, K., Hasegawa, Y., Gao, J., Ishihara, H., Shimosegawa, T., et al. (2005). Dissipating excess energy stored in the liver is a potential treatment strategy for diabetes associated with obesity. Diabetes *54*, 322–332.

Jezek, P., Zackova, M., Ruzicka, M., Skobisova, E., and Jaburek, M. (2004). Mitochondrial uncoupling proteins—facts and fantasies. Physiol. Res. *53* Suppl. 1, S199–S211.

Katagiri, H., Asano, T., Ishihara, H., Inukai, K., Shibasaki, Y., Kikuchi, M., Yazaki, Y., and Oka, Y. (1996). Overexpression of catalytic subunit p110alpha of phosphatidylinositol 3-kinase increases glucose transport activity with translocation of glucose transporters in 3T3-L1 adipocytes. J. Biol. Chem. *271*, 16987–16990.

Klingenberg, M., and Huang, S.G. (1999). Structure and function of the uncoupling protein from brown adipose tissue. Biochim. Biophys. Acta *1415*, 271–296.

Kopecky, J., Clarke, G., Enerback, S., Spiegelman, B., and Kozak, L.P. (1995). Expression of the mitochondrial uncoupling protein gene from the aP2 gene promoter prevents genetic obesity. J. Clin. Invest. *96*, 2914–2923.

Leonardsson, G., Steel, J.H., Christian, M., Pocock, V., Milligan, S., Bell, J., So, P.W., Medina-Gomez, G., Vidal-Puig, A., White, R., and Parker, M.G. (2004). Nuclear receptor corepressor RIP140 regulates fat accumulation. Proc. Natl. Acad. Sci. USA *101*, 8437–8442.

Matsuzawa, Y., Shimomura, I., Nakamura, T., Keno, Y., and Tokunaga, K. (1995). Pathophysiology and pathogenesis of visceral fat obesity. Ann. N Y Acad. Sci. *748*, 399–406.

Niijima, A. (1998). Afferent signals from leptin sensors in the white adipose tissue of the epididymis, and their reflex effect in the rat. J. Auton. Nerv. Syst. *73*, 19–25.

Ruan, T., Lin, Y.S., Lin, K.S., and Kou, Y.R. (2005). Sensory transduction of pulmonary reactive oxygen species by capsaicin-sensitive vagal lung afferent fibres in rats. J. Physiol. *565*, 563–578.

Scharrer, E. (1999). Control of food intake by fatty acid oxidation and ketogenesis. Nutrition *15*, 704–714.

Smith, G.P., Jerome, C., Cushin, B.J., Eterno, R., and Simansky, K.J. (1981). Abdominal vagotomy blocks the satiety effect of cholecystokinin in the rat. Science *213*, 1036–1037.

Tanida, M., Iwashita, S., Ootsuka, Y., Terui, N., and Suzuki, M. (2000). Leptin injection into white adipose tissue elevates renal sympathetic nerve activity dose-dependently through the afferent nerves pathway in rats. Neurosci. Lett. *293*, 107–110.

Tsukiyama-Kohara, K., Poulin, F., Kohara, M., DeMaria, C.T., Cheng, A., Wu, Z., Gingras, A.C., Katsume, A., Elchebly, M., Spiegelman, B.M., et al. (2001). Adipose tissue reduction in mice lacking the translational inhibitor 4E-BP1. Nat. Med. *7*, 1128–1132.

Um, S.H., Frigerio, F., Watanabe, M., Picard, F., Joaquin, M., Sticker, M., Fumagalli, S., Allegrini, P.R., Kozma, S.C., Auwerx, J., and Thomas, G. (2004). Absence of S6K1 protects against age- and diet-induced obesity while enhancing insulin sensitivity. Nature *431*, 200–205.